GLOBAL HEALTH PROJECT:
INFANT CARDIORESPIRATORY MONITOR

BME 400
Department of Biomedical Engineering
University of Wisconsin – Madison
December 12, 2012

Caleb Durante, Team Leader
Bradley Wendorff, Team Communicator
Don Weier, Team Webmaster
Drew Birrenkott, Team BSAC Representative
Mike Nonte, Team Treasurer

Advisor
Amit Nimunkar Ph.D.
Department of Biomedical Engineering
University of Wisconsin – Madison

Client
Engineering World Health
Amit Nimunkar Ph.D.
Laura Houser M.D.
Tiffani Diage

Table of Contents

Abstract

Sudden Infant Death Syndrome (SIDS) is the sudden, unexplained death of an infant under the age of one, usually while sleeping. While the national SIDS rates indicates a higher prevalence in developed countries, the lack of documentation and autopsies in third world countries has skewed this data. A more accurate portrayal of the situation worldwide is the number of neonatal deaths, or the deaths in the first four weeks of an infant's life. There are over four million neonatal deaths annually, with over 99% of these deaths occurring in low to mid income nations. Infant respiratory monitors have been shown to decrease the number of infant deaths while sleeping, but the current models on the market are cost prohibitive and to energy dependent to be an effective means of decreasing these tragic events in resource-scarce areas. To help reduce the incidence of SIDS in developing countries, specifically Ethiopia, a prototype infant respiratory monitor has been developed in semesters past utilizing impedance pneumography as its means of detection. The monitor has significantly reduced power consumption in addition to being less expensive than comparable devices, so it can feasibly be implemented in developing countries. A PIC18F14K22 has previously been selected as a low power microcontroller, and two rechargeable lithium ion batteries are integrated as the power source to allow for easy recharging. The ethical considerations concerning device reliability as well as patient and user safety were integral to the development of this device. This semester additional features are to be added, including heart rate detection and data logging capabilities. The powering system will be reduced from a dual supply to a single supply system for safety reasons. Furthermore, the low power PIC microcontroller will be replaced with a more computationally powerful Arm microcontroller to allow for more advance algorithms to be executed.

Background & Motivation

In 2000 the United Nations came up with a list of eight Millennium Development Goals (MDGs) and set the goal of achieving them all by 2015. The fourth of those goals was, “to reduce by two thirds, between 1990 and 2015, the under-five mortality rate,” (UNICEF 2012).

While there is still a lot of progress to be made in reaching this goal, the risk of a child dying within the first five years of life has been halved between 1960 and 1990 and continues to drop (Lawn et al 2005) (Figure 1). This pace however has not been similar across all under-five age groups, in particular, there has been very slow progress in reducing global neonatal mortality (Lawn et al 2005) (Figure 1). Estimates have shown that child mortality between the ages of two and five have fallen by about a third while the neonatal mortality rate (NMR) has dropped only by about a quarter (Lawn et al 2005). This means that a higher proportion of the under-five mortality rate is now due to neonatal mortality, and if the Millennium Development Goals are to be met, a successful means to lower the neonatal mortality rate must be implemented.

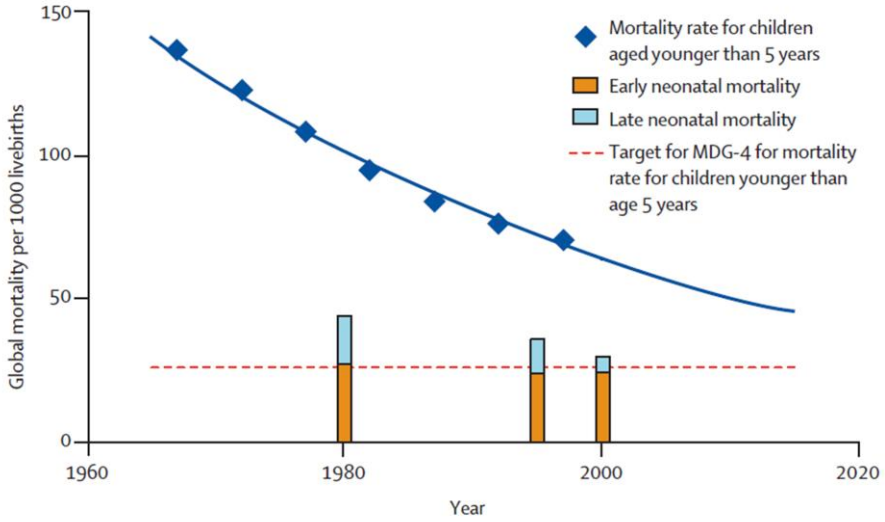

Figure 1: Actual and projected global mortality rate per 1000 live births in children under 5, early neonates, and late neonates, 1965-2015. Graphs indicate a drop in the mortality rate for children younger than five, but a much slower decrease for early and late neonatal mortality rates (Lawn et al. 2005).

The most effective way to devise a strategy of reducing NMR is to understand what is causing the NMR to be so high. Current research suggests that the problem is two-fold. The first problem is the inverse care law which states, “the availability of good medical care tends to vary inversely with the need for it in the population served,” (Lawn et al 2005). It has been observed that 99% of neonatal deaths arise in low-income and middle-income countries, but that the 1% of neonatal deaths that occur in high-income countries are the ones that receive the most attention and study (Lawn et al 2005). The second problem is that neonates are dying from conditions that are treatable and preventable. Studies have shown the three major causes of neonatal mortality to be

from three major causes: 36% from infections, 27% from preterm birth, and 23% from asphyxia (Lawn et al 2005) (Figure 2).

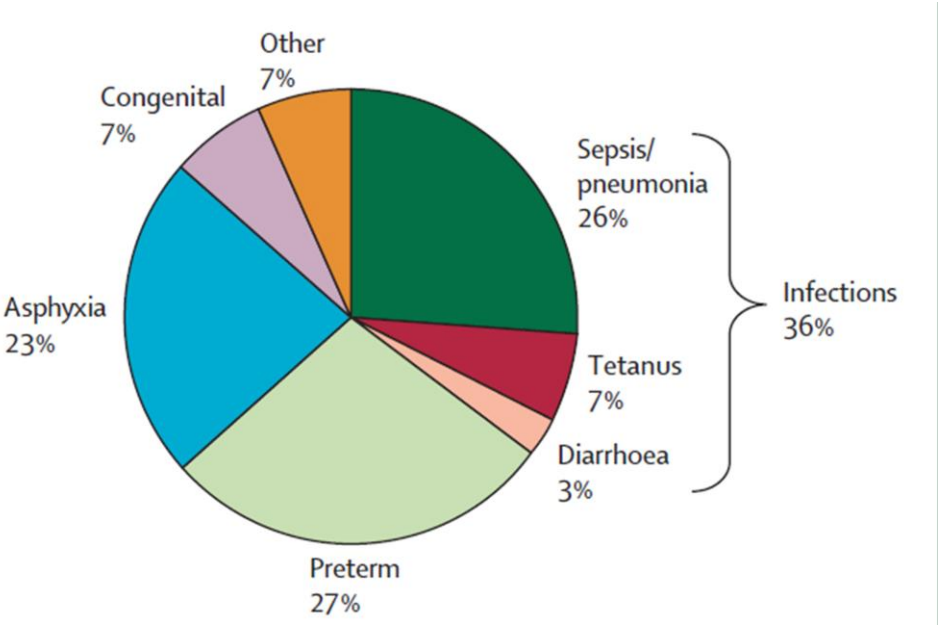

Figure 2: Estimated distribution of causes of neonatal deaths worldwide in 2000 (Lawn et al. 2005).

It is by looking at these two major problems in addressing neonatal mortality that our team draws our motivation. We are seeking to address these problems by developing a reliable, low-cost cardiorespiratory monitor to issue early warning alarms in the case of neonatal and infant apnea, asphyxia, or bradycardia that could easily be implemented in the countries where 99% of the neonatal deaths occur.

We believe that by doing this we will begin to address the problem of neonatal mortality. Our monitor will provide an adequate modality for monitoring neonates, and thus will address the inverse care law. In addition, our device will provide a warning system for neonates at risk for symptoms associated with asphyxia and preterm birth.

Pathophysiology

Two of the major causes of death of neonates that we seek to address with this monitor are asphyxia and preterm birth. While the two causes of death may seem to be quite different, the designations of these two groups can be misleading as both encompass a large number of pathologies, many of which are related to respiration. For example, one study in the United Kingdom found approximately 49% of deaths related to preterm births between 2002 and 2008 were due to respiratory ailments (Berrington et al 2012). Additionally, asphyxia has been associated with a number of pathologies including apnea and bradycardia in full term infants.

In discussing the pathology and physiology that results in a respiratory emergency in a neonate, we will focus on apnea. While there are a number of different reasons for a respiratory emergency, apnea is a common cause of death in both preterm and full-term neonates.

Apnea in its strict clinical sense is defined as the cessation of respiratory airflow for a length of time greater than 20 seconds (Rocker et al 2012). It is important to note that it is not uncommon for infants to undergo apneic events with duration less than 20 seconds during normal sleep, however, once the event exceeds 20 seconds it becomes a health concern (Marcus 2001). There are three types of apnea: central apnea, obstructive apnea, and mixed apnea (Rocker et al 2012).

Central apnea is associated with the nervous system and can result from a lack of stimulus by the central respiratory centers or the failure of the respiratory muscles or efferent peripheral nerves to process the nervous signals from the brain (Rocker et al 2012). Often this is seen in premature infants as these systems have yet to fully develop (Rocker et al 2012). Infants suffering from central apnea have no respiratory effort and thus will have no chest wall movement or breathing sounds (Rocker et al 2012). Obstructive apnea is caused by a blocked airway and is not signified by a lack respiratory effort (Rocker et al 2012). Obstructive apnea is associated with a number of other conditions including small airways or decreased strength in the pharyngeal dilator muscles (Rocker et al 2012). Mixed apnea is simply a combination of conditions from both central and obstructive apnea that together create a health risk (Rocker et al 2012).

Apnea can be used to explain many of the respiratory emergencies found in infants, but certainly not all of them. Unfortunately, the pathophysiology of each possible respiratory ailment cannot be covered here, but what is clear is that regardless of respiratory ailment, early resuscitation using a bag valve mask is of critical importance. One study found that a delay in the time of initiation in bag valve mask resuscitation resulted in more neonatal deaths. Infants that survived had a delay of 82+/-58 seconds while infants that died had a delay of 100+/-78 seconds (Ersdal et al 2011). Ultimately, this means that our monitor has a critical role to play because it can alert caregivers when an infant has stopped breathing and allow them to provide care more quickly and reduce respiratory related neonatal mortality, regardless of specific cause.

Our Area of Focus

The ultimate goal of our infant cardiorespiratory monitor is to be available at low cost for countries with the highest rates of under-five mortality and neonatal mortality. We currently have targeted two distinct countries to focus our efforts: Ethiopia and Haiti. These choices were made because both countries have demonstrated a great need for devices such as ours and two of our clients are working with doctors, nurses, and midwives who can ensure that our device is properly used. This will allow us to test its effectiveness for implementation on the broader scale.

Currently, both Ethiopia and Haiti have seen a drop comparable to the global average in under-five infant mortality rate, but suffer from neonatal mortality rates that are still very high. (UNICEF 2012, Lawn et al 2005) (Figure 3). Currently, neither one has reached the 2015 Millennium Development Goal, but with a strong effort to reduce the neonatal mortality rate, the goal is within reach for both nations.

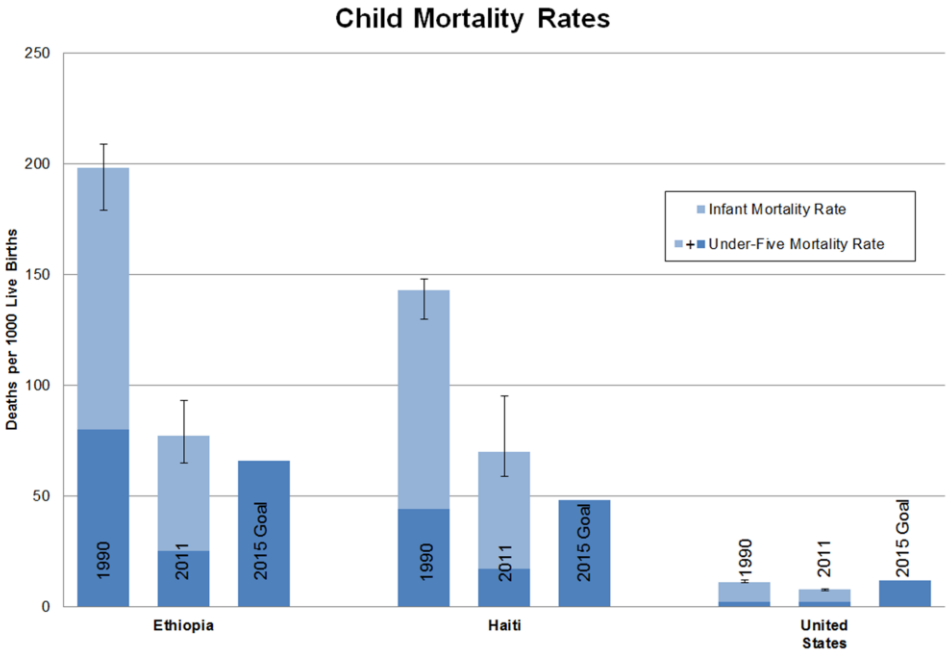

Figure 3: 1990, 2011, and 2015 MDG-4 for under-five mortality rate and infant mortality rate in Ethiopia, Haiti, and the United States (UNICEF 2012).

Current Methods

There are many devices that are currently on the market that provide monitoring systems for infants while they sleep in an in-home setting. Typically, these monitors ensure that infant respiration rates maintain steady levels on a per minute basis, and that cessation of breathing does not occur. There are many ways to monitor respiration including impedance pneumography, which measures changes in chest cavity resistance during breathing (Grenvik, 1972). Pulse oximetry can also be used to monitor respiration rates by measuring oxygen levels in the bloodstream. Force plates are another form of respiration monitoring, and they monitor infant motion artifacts and sound an alarm in motion absence of more than twenty seconds (SUDC.org, 2012). A fourth way of monitoring infant respiration is using temperature sensitive thermistors to measure temperature fluctuations consistent with inhalation and exhalation and the heat content of the surrounding air (Norman, 2012).

The first competitive respiratory monitor currently on the market is the Babysense II (Figure 4), which utilizes two large force pads placed under the crib mattress to sense if the infant is breathing properly. The Babysense depicts a green, 'all-clear', light when the infant is breathing normally, but emits an audible alarm if the infant's respiration rate decreases to less than ten breaths per minute or breathing ceases for more than twenty seconds. The monitor is powered by standard AA batteries and costs $279.00 per unit (Hisense Ltd. 2012).

Figure 4: The Babysense II Monitor detects breathing motion through the use of a force mat (Hisense Ltd., 2012).

Another respiratory monitor available for home use is the Angelcare 201 model (Figure 5). This monitor also uses a force mat that is placed under the crib mattress to monitor the infant during the night. The Anglecare model sounds an alarm when the infant stops breathing for more than twenty seconds. The power source for this monitor is an AC adaptor as well as a battery backup for use in the case of a power outage that requires eight AA batteries. The cost of the unit is $129.99 (Angelcare Monitors Inc., 2012).

Figure 5: The Angelcare 201 monitor, like the Babysense II Monitor, uses a force mat to detect forces that indicate breathing (Angelcare Monitors Inc., 2012)

The Respisense baby monitor differs from the previous two monitors mentioned in that it uses a motion detection method of monitoring respiration rates (Figure 6). The device clips onto the infant's diaper, which allows for supervision away from the crib, which a permanent force mat does not allow. After twenty seconds of inactivity, the sensor alerts the caregivers with a built-in alarm system. The system also tickles the infant's stomach if movement ceases for fifteen seconds. The price for the Respisense monitor is $100 (Infantrust, 2012).

Figure 6: The Respisense monitor attains mobility by clipping directly to an infant's diaper, and senses breaths by measuring pressure between a baby's belly and the waistband of the diaper (Infantrust, 2012).

While these systems are compatible for use in developed countries, all three models present obstacles for use in a mobile clinic setting, where resources are scarce and a consistent source of batteries is limited. The recurring cost and difficulty of obtaining batteries in the Babysense and Respisense monitors is too high, and the lack of consistent electric power in mobile clinics eliminates the Angelcare (AC adapter) from consideration (Infantrust, 2012). In addition, the devices described have an overhead cost that can be prohibitively expensive for use in a mobile clinic. After examining the currently available respiration monitoring techniques, our team opted to use what we believe is a more sustainable detection method for developing countries—impedance pneumography.

Impedance Pneumography

Impedance Pneumography uses the changing resistance through the thoracic region to track respiration. By passing a carrier wave through the trunk of a patient, and comparing it to the output wave on the opposite side of the trunk, an amplitude modulated sine wave is produced, where sections of higher amplitude correspond to inhalations and vice versa. By passing the wave through a demodulating envelope rectifier, a sine wave that corresponds to breathing can be produced. A block diagram of the method can be seen in figure 7.

The resistance that is encountered at the skin path stage of the method is a summation of skin resistance, which is “fixed” on short time scales, but can be susceptible to drift overtime based on skin moisture as well as other factors. Impedance below the skin is increased during inhalations because the path length is increased, and because air is more resistant than tissue. Since the variation in thoracic impedance is small when compared to skin resistance, a high gain needs to be applied to the differential amplification stage for a useful wave to be produced.

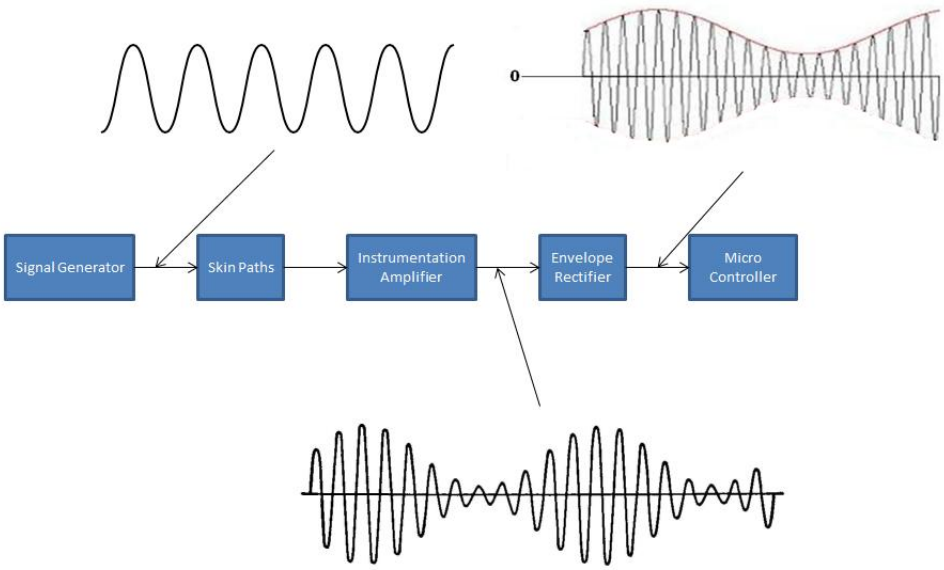

Figure 7: Impedance pneumography uses a carrier wave, differential amplification, and demodulation as shown here. The resulting waveform can be read by a microcontroller and algorithms can be applied that will determine if breathing has taken place.

Problem Statement

The goal of this project is to produce an infant apnea monitor that will detect and alert a caregiver after an infant between 0 and 12 months has stopped breathing for more than 20 seconds. The device's intended environment will be in disaster stricken or developing regions of the world. Thus, the unit must be very inexpensive and its ease-of-use is of the utmost importance. Additionally, the device must still maintain high levels of durability, reliability, and safety in accordance with governing regulatory agencies.

Client Requirements & Design Constraints

The primary function of the device is to effectively alert nearby caretakers in the event that the infant ceases breathing for more than 20 seconds. Therefore, the device must be capable of monitoring an infant's breathing pattern and alert nearby caretakers via audio and/or visual alarm if breathing is not detected for 20 seconds. The device must be highly reliable and consistent, since a failure of the device could result in the death of an infant. Because a failure to detect breathing cessation could have fatal consequences, the device should be designed to be more oversensitive than under sensitive, as false negatives pose a greater threat than false positives. However, if the device sounds too many false alarms, caretakers may begin to dismiss it, therefore device accuracy is important. The device must be safe to use both for the infant and operators. It cannot interfere with healthy electrical signals in the infant, nor pose the risk of shock to the infant or caretakers. Any external wiring used must not present a risk of strangulation or entanglement to the infant, and there should be no small, easily breakable parts that could present a choking hazard. The device must allow for comfortable, normal sleep for the infant. Any device components that come in contact with the infant must receive sterilization between uses. In designing the device with the operator in mind, it must be simple to use and easy to operate with minimal training. As a medical device, the device must meet all regulatory demands outlined by the government and other agencies. Therefore, it must comply with HIPPA and patient disclosure standards, as well as receive FDA approval.

A portable device must be small with a maximum size of 10 cm x 10 cm x 10 cm and a maximum weight of 1.0 kg. The device should weigh at least 200g to prevent it from being easily knocked off a table, stand, etc. The device must be robust and able to withstand reasonable wear due to use. Since acquiring replacement devices or pieces and performing repairs on the device may not be an option for organizations using the device in the field, the risk of broken parts must be minimized. The device should have a long shelf life, with the only regular maintenance needed being replenishing the power supply from time to time. This power will be provided by a battery, since power grids in many of the intended environments of operation are often either unreliable or non-existent. Ideally the power source will require minimal replacement and/or recharging, and so in addition to having a long lasting reliable power source implemented into the device, the device itself must be as power efficient as possible. Therefore, the device should operate on 70 mA or less.

The aim of this project is to produce a functional prototype unit to prove manufacturability. The cost of the device must be kept low, due to the nature of the project. Therefore, the target cost per unit is a maximum of $30. Device components will include basic circuitry such as resistors, capacitors, and amplifiers, wiring, a microprocessor, instrumentation amplifiers and standard op-amps, a battery, a speaker, electrodes, and housing. A more detailed product Design specification can be seen in appendix A.

Design Options & Selection Matrices

Microcontrollers

While many powerful microcontrollers are available for device development, including the Hitachi SuperH, Analog Devices ADuC, and Intel 8051, we have narrowed our selection process down to the PIC family from Microchip and the AVR family from Atmel. We made this decision based on the fact that we already have development boards available for these microcontroller families; development boards can cost up to $200, so this decision reduced the cost of development (Atmel, 2012). The quality of our design did not suffer from this decision, as both microcontroller families contain a wide range of models with hardware that meets our basic needs for this project and both have a large online support community.

Our basic hardware requirements for the project are: analog-to-digital converter (ADC) with sample rate of at least 100ksps, pulse-width modulation (PWM) with output speed of at least 30 KHz, serial communication interface capability, timer interrupt capability, and flash memory expansion capability. As stated previously, the AVR and PIC families both offer microcontroller models fulfilling these minimum hardware requirements (Atmel, 2012) (Microchip, 2012). The AVR and PIC families differ in some aspects such as the complexity of the instruction set and the size of instructions, but for the requirements of this project, they are nearly functionally identical.

Two areas in which the microchip families do differ that are relevant to the performance of this device are the working memory and sleep modes. The AVR family has 32 working registers while the PIC family has one working register. Working registers store intermediate values created during calculations; values that do not fit in the working register are backed up to memory. The advantage of having a larger number of working registers is that a larger number of variables can exist simultaneously without having to be backed up to memory; this increases the speed of calculations. Since we are planning to increase the complexity of our detection algorithm by adding volume and slope variables, we will need to keep track of a larger number of variables. It would therefore be advantageous to use the AVR family since this will allow a greater computation speed. Sleep states are used to turn off the system clock when the device does not need to be active to conserve power. The PIC family offers a slightly more power efficient sleep mode than the AVR family. Power consumption is a concern in this project because the device will run on battery power.

When developing a device with and embedded microcontroller, a development board is an essential tool. Development boards allow the user to program the microcontroller program memory, and check that the microcontroller performs properly before integrating it into the device. We have received the permission of the mechatronics lab to use their STK600 development boards, which are designed to be used with Atmel microcontroller families. The BME department also has custom development boards available for the PIC microcontroller family. Another resource that can be useful when developing an embedded system is an on-the-chip debugging tool. These tools allow the user to step through program code one line at a time while observing changes in variable value and I/O values; this can allow the user to find problems that might otherwise be hidden due to the high speed of code execution. The

mechatronics lab has given us permission to use the JTAG-ICE mkII debugging tools for the Atmel microcontroller family. While the PIC family has on-the-chip debugging tools available for purchase, we do not have access to any of these tools.

Integrated development environment (IDE) software is a useful tool for programming a microcontroller. Atmel Studio 6 and MPLAB 8 are two free IDEs for Atmel and Microchip microcontrollers, respectively. Both IDEs offer an integrated C-compiler. Atmel Studio 6 offers over 1,000 pre-written code examples to help developers get started on their project. An additional software resource we have for the AVR family is CodeVisionAVR. This software program is available through CAE and features a CodeWizard tool that automatically generates code for Timers, ISRs, I/O setup, and many other peripheral settings. The use of such a tool would greatly reduce the time needed to develop and edit code, and thus would greatly reduce the length of the design cycle.

While our current device prototype uses a PIC microcontroller and the PIC family offers a more power efficient sleep mode, we have chosen to use the Atmel AVR family for our final device. As can be seen in the microchip selection matrix, PIC and AVR families are matched in hardware and community support. Ultimately, we felt that the ease of code development and code debugging capabilities of the AVR family outweighed the slight reduction in power efficiency.

Table 1: Design matrix quantifying the weighting of each category considered in choosing a microcontroller, and how the Atmel AVR chip and PIC microcontroller scored in each category

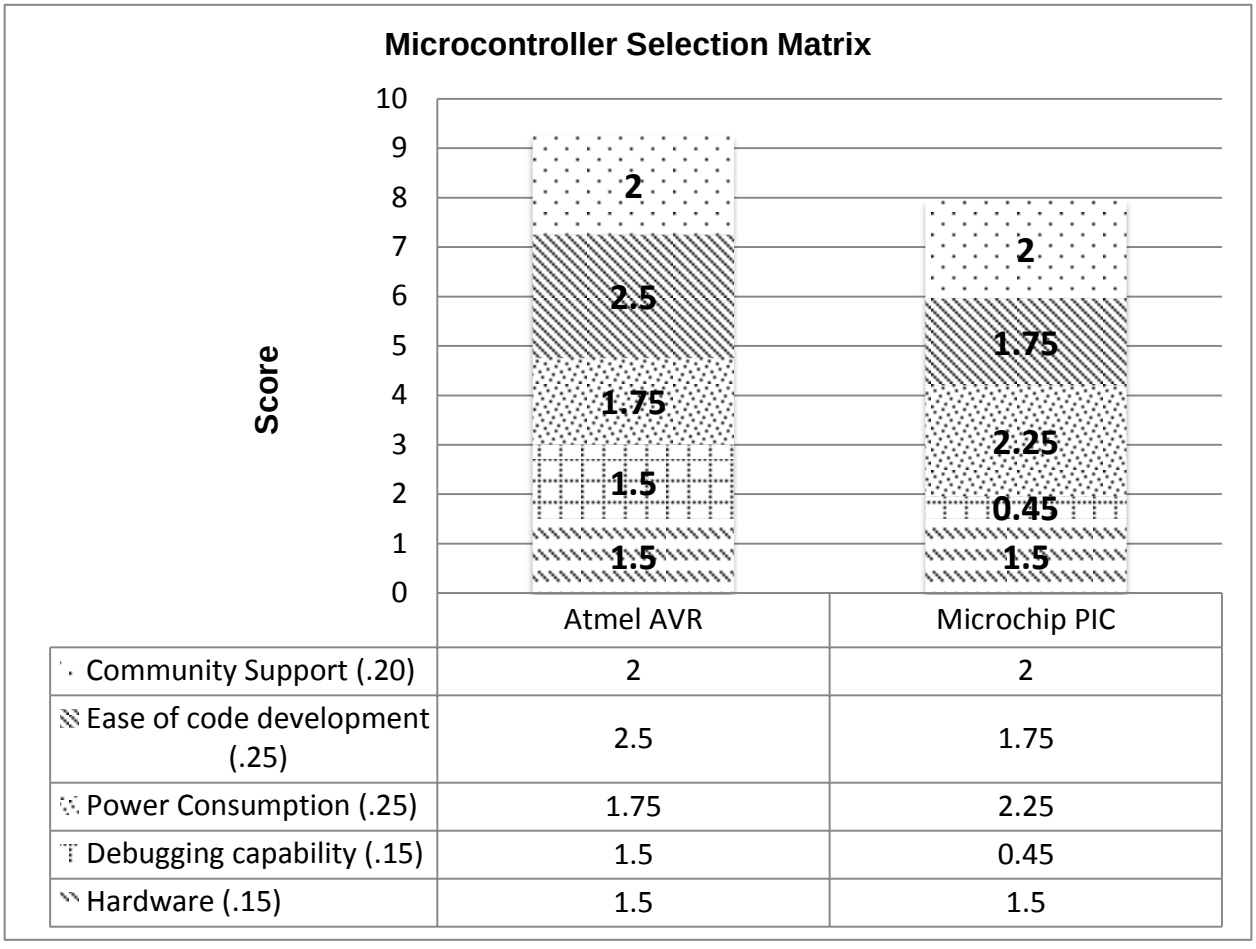

	Atmel AVR	Microchip PIC
Community Support (.20)	2	2
Ease of code development (.25)	2.5	1.75
Power Consumption (.25)	1.75	2.25
Debugging capability (.15)	1.5	0.45
Hardware (.15)	1.5	1.5

Electrode Selection

Design Constraints

As the only part of the monitor that will actually be in contact with the patient, the selection of the electrodes for the monitor is of critical importance. In the current design, the lead system we are incorporating will include four separate electrodes. One will serve as the carrier electrode, which will be connected to the output of the carrier generation circuit. This signal flows into the body and through an adjacent electrode that is connected to ground. The other two electrodes will be used to measure the signal amplitude at different points along the thoracic cavity. Based on this system, two commercially available electrodes types were considered and evaluated when deciding which electrode would be most suitable for this monitor—carbon/rubber electrodes and Ag/AgCl electrodes. To determine which electrodes are best for this application, four factors are considered for effectiveness and also the conditions under which the electrodes will be used. Each factor was given a weight out of a total weight of 1.0. These four factors (and their weight) are: reusability (0.5), cost (0.3), sensitivity (0.15), and allergen risk (0.05). An explanation of each factor and the rating that each electrode type received, and why, follows below.

Reusability

The most critical factor for our selection of electrodes was the reusability of the electrodes we chose. All available evidence suggests that if the electrodes the monitor is designed to use are one time use, the monitor will be used until the electrodes run out, and then will not be used again. This does not suggest a sustainable system to us or one that really works to address our ultimate goal of reducing the neonatal infant mortality rate. Of the two electrode systems considered, only one really fit this requirement—the carbon/rubber electrodes.

The vast majority of Ag/AgCl electrodes are one-time use. In our case they would be used for one night and then disposed of. There are a few examples of Ag/AgCl electrodes on the market that are termed “reuseable” however this often means they can be used reused upwards of seven to ten times before being replaced. Ultimately though, they suffer from the same problem as single use electrodes (Luo et al 1992). The Ag/AgCl electrodes were given a final rating of one out of ten because they don’t meet the criteria, but they were not given a zero because there are a small number of available electrodes that could perhaps be considered semi-reusable.

Conversely, the carbon/rubber electrodes are truly reusable. In testing they are held in place using elastic bands or tape, can be removed and sterilized, and reapplied to the same or a different patient (Luo et al 1992). These leads, if properly cared for, are truly reusable, and received a rating of eight out of ten. They however did not score perfectly because over a long period of time they will wear out and need to be replaced. For all intents and purposes, they are the most reusable electrodes available on the market.

Cost

Another very critical factor in the design of the electrodes that was considered was the cost which received a weight of 0.3 out of 1.0. This factor was weighted so

heavily because the goal of this monitor is to be implemented in developing regions where often the daily wage is below $10.00 per day (Chen and Ravallion, 2008). Therefore, the more cost effective every element of the monitor, the more realistic its mass implementation will be.

The most commonly used Ag/AgCl electrode is the 3M Red Dot®. The average cost of one 3M Red Dot® electrode is approximately $0.50 per electrode for the average consumer (www.amazon.com). If four of these electrodes were required per day and the monitor was used every day, this would correlate to a total cost of $730.00 per year. In comparison, the carbon/rubber electrodes have an average cost of $10.00 per electrode (www.amazon.com). Reusable electrodes thus incur to a total cost of $40.00 per year.

Both of these costs were obtained off of a commercial site and it can be expected that the cost of both of these electrode types would be significantly reduced when they were purchased in large quantities. The comparison however is obvious, simply because so many of the Ag/AgCl electrodes would be required per year; therefore the price will easily outpace the cost of the reusable electrodes. The Ag/AgCl electrodes were given a score of two out of ten and the rubber electrodes were given a score of eight out of ten.

Sensitivity

The third design factor considered was sensitivity. This factor was given a weight of 0.15 out of 1.0; much smaller than the previous two factors. Electrode sensitivity does not constrain our design to the degree that reusability and cost do. This is because signals acquired by insensitive electrodes can be filtered, amplified, and ultimately "designed around". This factor is still very important and must not be taken lightly or overlooked, as picking sensitive electrodes will only make the design process easier.

Again in this category, there was a clear electrode type that performed best, but it was not the carbon/rubber electrode. The sensitivity of electrodes is often measured as the signal-to-artifact ratio (SAR). The SAR is amount of noise in the signal that in our case would be returned to the monitor to be evaluated (Luo et al 1992). A study looking at a number of different electrode types ultimately concluded that adhesive-gel electrodes were preferred to rubber electrodes, because even using tape and tight elastic bands, the SAR was far from ideal for the rubber electrodes (Luo et al 1992). The SAR for rubber electrodes was so great that they were not even considered in a follow-up study looking at pediatric electrodes (Mayotte et al 1994). Due to these reports the Ag/AgCl electrodes were given a rating of nine out of ten and the carbon/rubber electrodes were given a rating of two out of ten.

Allergen Risk

The final design factor for the electrodes that was considered was the allergen risk of both types of leads. This was given a weight of 0.05 out of 1.0. This factor is important to consider, but was not given a large weight. This is because both electrodes are commercially available, indicating that for the most part they are clinically used and thus the allergen risk is low. The two electrode types considered were both given a score of seven out of ten.

Design Matrix

Table 2: Design matrix quantifying the weighting of each category considered in choosing electrodes, and how the carbon/rubber electrodes and the Ag/AgCl electrodes scored in each category

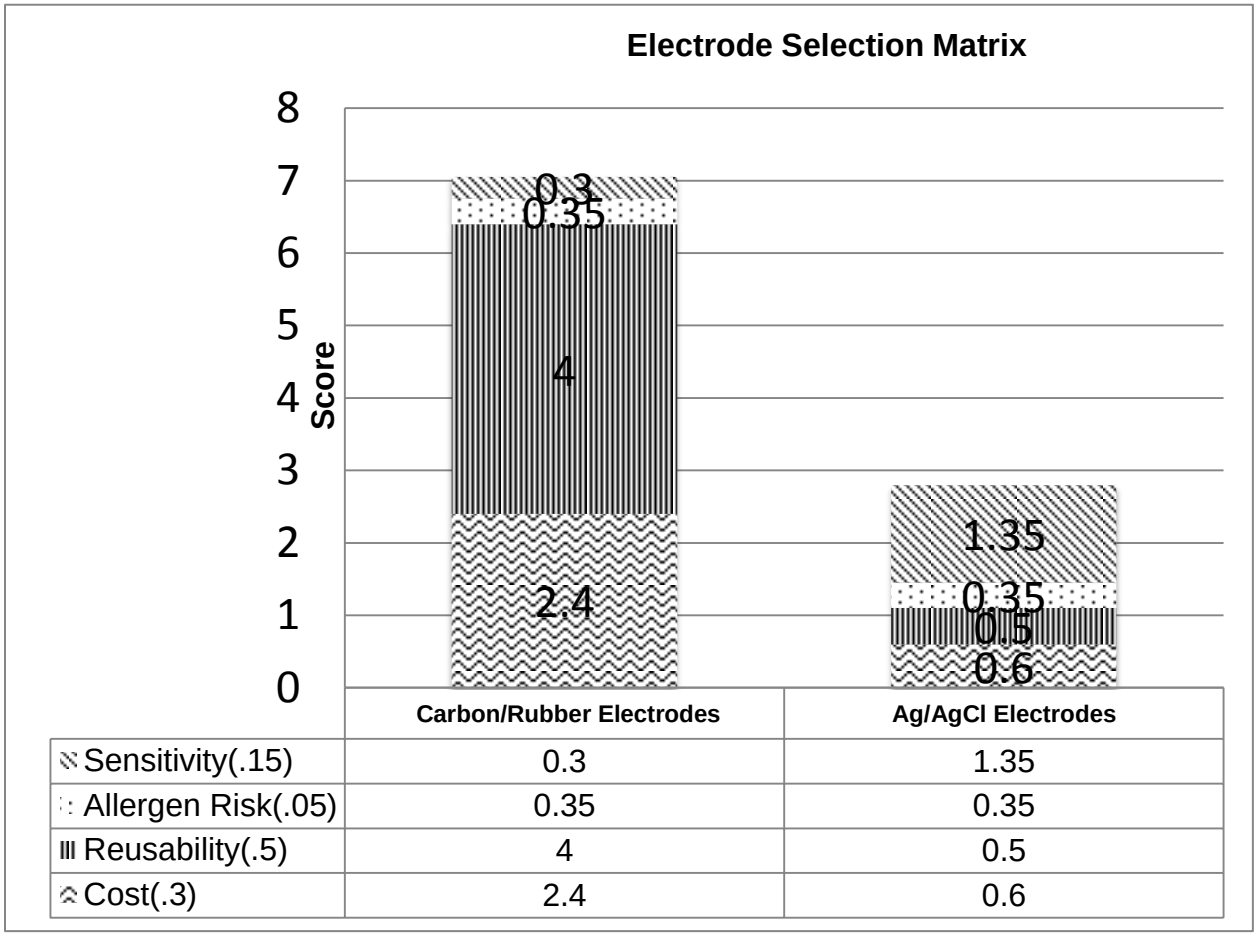

	Carbon/Rubber Electrodes	Ag/AgCl Electrodes
Sensitivity(.15)	0.3	1.35
Allergen Risk(.05)	0.35	0.35
Reusability(.5)	4	0.5
Cost(.3)	2.4	0.6

Based on these scores and the weights assigned to each factor a design matrix was created by multiplying the score out of ten each electrode got for each factor by the factor weight and adding all of the factors together (Table 2). Due to the heavy weighting of reusability and cost, the carbon/rubber electrodes scored much more highly (7.05) than the Ag/AgCl electrodes (2.8).

The results of this matrix however are a little unsettling especially since the use of carbon/rubber electrodes poses a risk for very high SAR in the final design. In order to combat this, a number of modifications will be considered in order to use the carbon/rubber electrodes but ensure that their sensitivity is of a high enough quality to meet clinical standards. Four different electrode-specific factors will be considered in order to create the highest SAR for the carbon/rubber electrodes. These factors are: electrode size, electrode placement, conductivity solution, and electrode to body attachment.

In at least two reports in which electrode size was considered, it has been found that the larger the size of the electrode, the larger the SAR is (Mayotte et al 1994, Luo

et al 1992). In testing this factor the size of an infant and the risk of the electrodes touching will be balanced with electrode size to yield the largest electrodes possible. Electrode placement has also been considered in previous studies in adults where it was found that the most effective electrode placement was directly over the sternum on the upper back approximately on the T5 vertebrate (Luo et al 1992). This however will need to be tested and confirmed in infants as well as altered to account for the use of four leads as opposed to the two lead system used by Luo et al (1994). The third factor will be the use of a conductivity solution for use with the carbon/rubber electrodes. It was found that the SAR was greater in carbon/rubber electrodes when a saline solution was used (Luo et al 1992). Based on this finding, a conductive solution will be designed that is conductive to better adhere the electrodes. Additionally, the conductive solution will be fabricated out of items that are commonly available in developing countries such that it can be re-made when it runs out. Finally, the attachment of the electrodes to the body will be studied. The will be placed within an elastic band that has both a strap around the chest cavity. It is the hope that by securely fastening the electrodes to the body, the artifact due to electrode slippage on the body can be reduced.

Ultimately, the best choice in electrodes for this monitor was the carbon/rubber electrodes because of their reusability and cost. However, in further consideration of the required sensitivity, it is the goal to modify the conditions in which these electrodes will be used to create the most sensitive and effective electrode system.

Final Design

Hardware Specifications

Power Supply

A single Lithium-polymer rechargeable battery will be used to power the device. These batteries are similar to those found in cell-phones and other portable electronic devices available today. A typical 3.7 Volt LiPo battery can hold approximately 2200 mAH of current, which makes them ideal for a continuous monitoring device. The majority of the components in the subsequent analog instrumentation circuit require a supply voltage of 5 Volts, and thus a 5 V boost regulator will also be implemented in the power supply functional block.

To facilitate controlled recharging of the LiPo battery, without the need to physically remove the battery from the device, an onboard recharge circuit will be included capable of recharging at a rate of 500mA/H. The power circuit will also include an under-voltage protection block that functions to interrupt the connection between battery and circuit in the event that the available voltage from the battery falls below 2.6 Volts. This feature is critical to ensure the long-term quality of the device by removing the possibility for component damage caused by an insufficient voltage source.

With the aforementioned design requirements in mind, the device will implement power supply circuitry of the Power Cell – LiPo Charger/Booster (PRT-11231) from Sparkfun electronics. (Figure 8)

Figure 8: Power Cell – Lithium Polymer rechargeable battery charger and boost regulator. Capable of sourcing up to 600mA @ 5V. (sparkfun.com)

Analog Instrumentation

Carrier Generation

Impedance pneumography operates by extracting the amplitude modulation signal of a known high-frequency carrier wave that is injected across the chest. This carrier signal will be generated by a connection of operational amplifiers with positive feedback causing unstable oscillation between the power rails. The circuit depicted in figure 9 produces a true analog sine (as opposed to cosine) wave when V_{out} is attached to the second output of the quadrature oscillator.

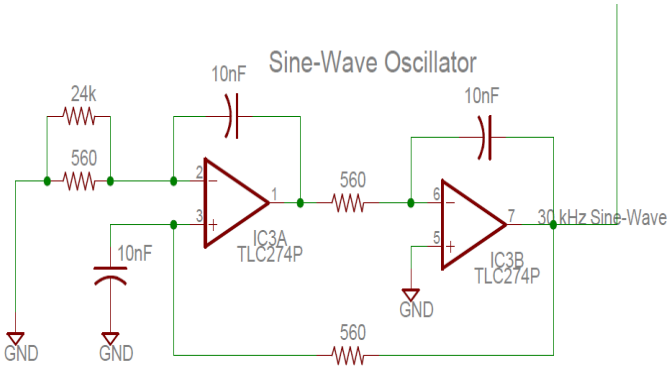

Figure 9: Quadrature Oscillator – An unstable connection of operational amplifiers causes periodic switching between the two power rails. In this case, the frequency of oscillation is determined by $f = 1/(2\pi RC)$, and amplitude is controlled by the parallel combination of 24 kΩ & 560 Ω

Patient Isolation

Proper patient isolation is commonly accomplished by integrating transformers or optocouplers between the patient and device. Though both transformers and optocouplers provide effective isolation, optocouplers will be used in the design, as they rely on LED light to transmit an electrical signal, and therefore emit no electromagnetic interference (and can't be interfered with by other EMI emitting devices nearby), as is characteristic of a transformer. A simple block diagram illustrating the location of the optocouplers with reference to the patient can be seen in figure 10.
Optocouplers surround the patient at input, and output, as well as between the analog and digital components of the device, which ensures that the microcontroller will also remain functional in the event of an electrostatic discharge or power surge.

Figure 10: Functional block diagram illustrating the position of optoisolators in the circuit.

In choosing an optocoupler, the working voltage of the device must be considered, as it dictates the necessary creepage and clearance distances of the component. Creepage distance is defined as the shortest surface path over a solid dielectric between two galvanically isolated conductors; likewise, clearance is shortest distance through the air. At or below a working voltage of 17 V_{DC}, or 12 V_{rms}, optocouplers providing reinforced insulation have a creepage distance of 3.4 mm and a clearance of 1.6 mm (Been, 2007).The IL300 Linear Optocoupler by Vishay Semiconductors meets the requirements for reinforced isolation, and is currently the component of choice to ensure patient isolation. Three IL300's will be integrated in the circuit in accordance with the block diagram in figure 10**.**

Instrumentation

An instrumentation amplifier subtracts the voltage present at the ground side of the chest from the voltage present at the carrier side of the chest synchronously. The difference is then amplified by a gain factor, which is controlled by a single resistor '*Rg'*. The resultant waveform is an amplitude-modulated version of the original carrier signal as shown in figure 11. By Ohm's law, the peaks of the AM signal correspond to points of full inhalation and the valleys correspond to the moments of complete exhalation. The amplitude values at these points of inflection are of significant importance to the apnea detection algorithm, and will be discussed in subsequent sections. In addition to modulation due to respiration, the electrical activity of the heart also modulates the carrier signal. The result is a respiratory sinusoid with a superimposed ECG.

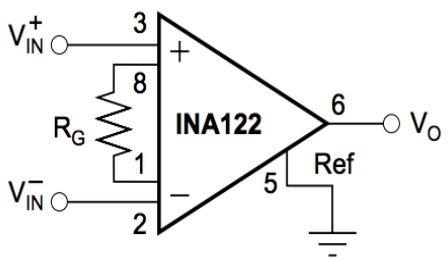

Figure 11: Instrumentation Amplifier – Texas Instruments INA122. Vo = G[(Vin+)-(Vin-)] where:

$$G = 5 + \frac{200k\Omega}{R_G}$$

(Taken from www.ti.com)

Amplitude Demodulation

Demodulation is accomplished by a precision full-wave rectification block that takes the absolute value of the AM signal by passing it through an operational amplifier configured as a superdiode. The resulting positive signal is then passed through an envelope detector, which extracts the modulation signal from the waveform. This smooth, periodic, signal corresponds to the change in chest impedance as a function of respiration, and is the signal of interest. In figure 12 the parallel combination of R1 and C1 is selected such that $1/(2\pi R_1 C_1) << f_{carrier}$. This allows capacitor C2 to store the peak charge of the envelope without fully discharging before the next voltage peak of the envelope.

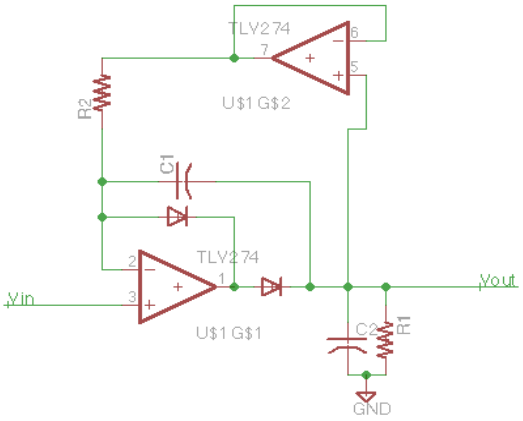

Figure 12: Amplitude demodulation block. A precision full-wave rectifier followed by an envelope detector accomplishes AM demodulation. The envelope detector will extract the positive envelope of the signal provided that $1/(2\pi R_1 C_1) << f_{carrier}$

AC Coupling and Analog Filtering

The envelope of the AM signal contains a DC-offset that is equal to the voltage drop caused by the patient's baseline chest impedance at full-exhalation. To prevent ADC saturation, and to improve the resolution of the signal at the input to the microcontroller, it is imperative that the signal be AC-coupled to remove this DC-offset.

A high-pass filter configured to have $f_c = .05$ Hz removes the DC-offset of the signal and also prevents the signal from drifting away from a provided analog reference value in the event of motion artifacts of changes in patient orientation. A low-pass filter configured to have $f_c = 17$ Hz will sufficiently attenuate high frequencies (including noise contributed by 60 Hz power line interference) without attenuating the respiratory rate signal or the QRS complexes of the ECG (Tompkins, 1993). The combination of these two filters is a band-pass filter with bandwidth .05 Hz – 17 Hz and some gain value determined by resistive combination R_f/R_i. At this point the signal is conditioned enough to be fed into the ADC of the microcontroller for sampling and processing.

QRS Detection

Figure 13 shows schematic for the QRS detector consisting of the following five subunits:

1. Band-pass filter. The power spectrum of a normal ECG signal has the greatest signal-to-noise ratio at about 17 Hz. Therefore to detect the QRS complex, the ECG is passed through a band-pass filter with a center frequency of 17 Hz and a band-

width of 17 Hz. This filter has a large amount of ringing in its output (Tompkins, 1993).

2. Half-wave rectifier. The filtered QRS is half-wave rectified, and subsequently compared with a threshold voltage generated by the detector circuit.
3. Threshold circuit. The peak voltage of the rectified and filtered ECG is stored on a capacitor. A fraction of this voltage (threshold voltage) is compared with the filtered and rectified ECG output.
4. Comparator. The QRS pulse is detected when the threshold voltage is exceeded. The capacitor recharges to a new threshold voltage after every pulse. Hence a new threshold determined from the past history of the signal is generated after every pulse.
5. Monostable. A 200-ms pulse is generated for every QRS complex detected. This pulse drives an indicator LED.

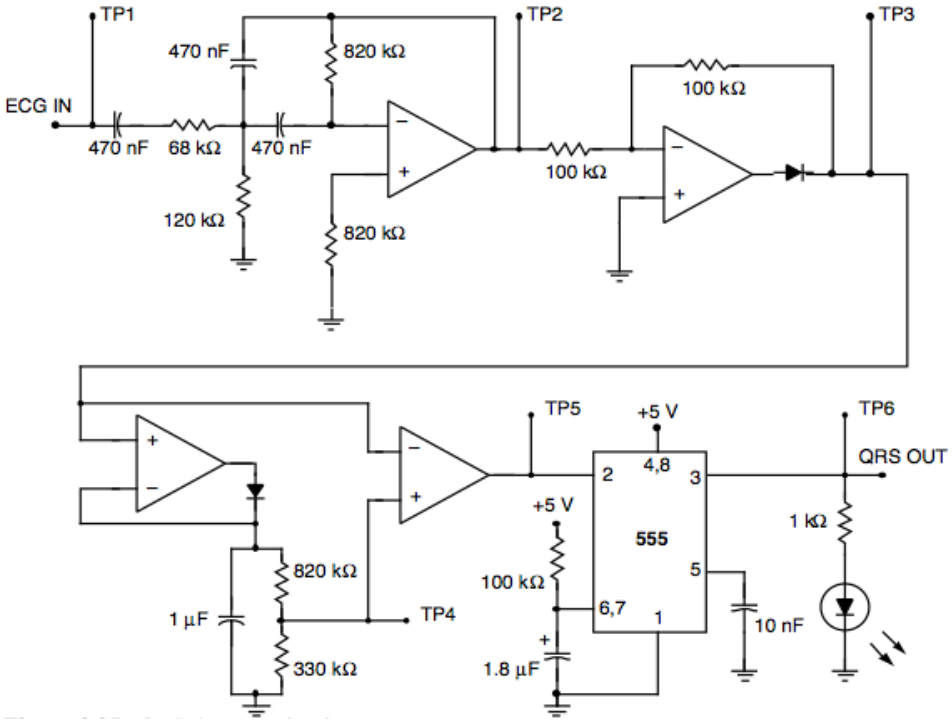

Figure 13: QRS Detection Circuit – Optional QRS filter (TP1-TP2), Half-wave rectifier (TP2-TP3), Threshold Circuit (TP3-TP4), Comparator (TP4-TP5), Monostable (TP5-TP6). (Tompkins, 1993)

The monostable pulse is connected to an input pin on the microcontroller which counts the pulses and can thereby calculate a real-time value for average heart rate to serve as a backup metric for alarm in the event the apnea detection algorithm fails to signal the presence of an adverse event.

Microcontroller

Before choosing a microcontroller, we outlined minimum required hardware and software needs. These specifications are discussed above in the design options and selection matrices section. Based on previous experience with embedded software development and the advice of engineering faculty members, we chose to prototype our software on a microcontroller that exceeds our minimum required specifications. This has allowed us to focus on proving that a microcontroller is capable of performing our required digital signal processing and apnea detection tasks without the need to spend time optimizing code to run on a less powerful microcontroller. When developing embedded software, it is necessary to have a prototyping platform that can power, program, and communicate with the microcontroller. We selected the Arduino Mega 2560 as our microcontroller prototyping platform because of its low cost and large online support community. The Arduino Mega 2560 uses an atmega2560 microcontroller; the specifications for this microcontroller more that meet our needs and are contained in appendix B.

Software Specifications

Programming of the atmega2560 microcontroller on the Arduino Mega 2560 was performed using a JTAGICE mkII debugging tool connected to the board's ISP header. Figure 14 shows a block-diagram representation of the software. After the device is turned on, it waits for a push button to be pressed by the user. This push button begins the calibration loop in which the patient's breathing is recorded and maximum and minimum peaks are determined. After 40 seconds of calibration, an average max-min peak difference is calculated. After calibration has completed, the device's alarm is enabled and patient monitoring begins.

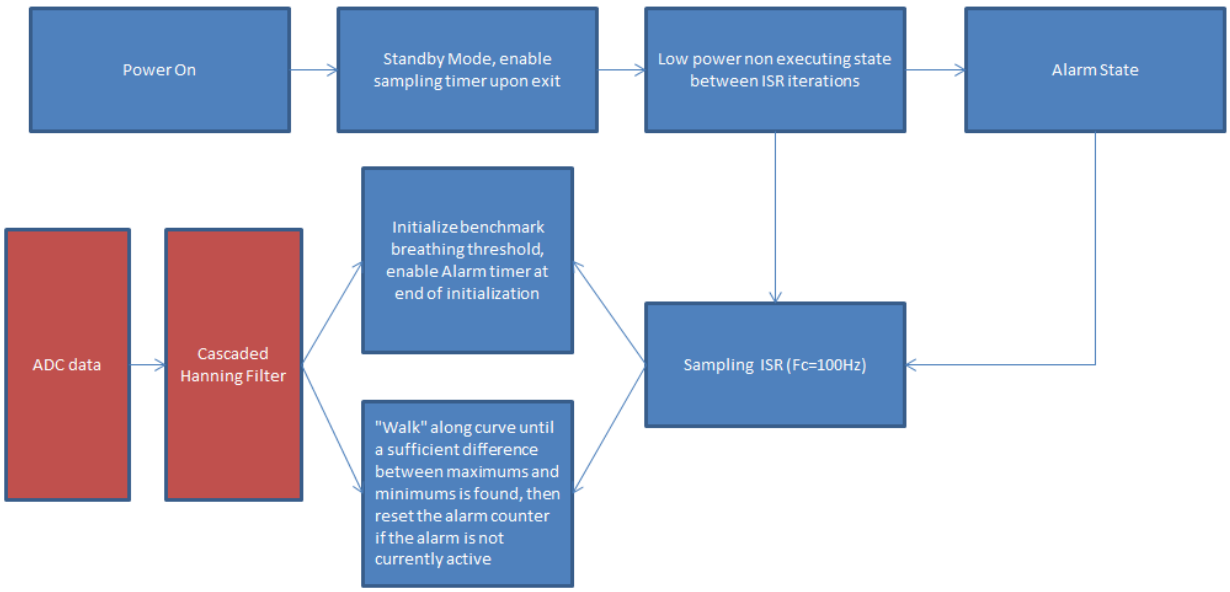

Figure 14: Functional Block Diagram of the Software Design.

During monitoring, the voltage input to the microcontroller is sampled at 100 Hz by the on-board ADC. This signal is split into two filtering pathways. Figure 15 shows a block-diagram representation of the two filtering pathways: one for the breathing waveform and one for the heartbeat detection. The breathing waveform filtering path begins with the signal being resampled to 10 Hz; this does not remove any useful information since the upper threshold for breathing frequency is less than 5 Hz (the Nyquist frequency when sampling at 10 Hz). Next the signal is passed through a finite impulse response (FIR) Hanning filter to smooth the waveform. The first step in the heartbeat detection signal processing path is an infinite impulse response (IIR) filter. This filter removes the low frequency breathing component of the signal and unnecessary. Next the absolute value of the signal is taken to increase the magnitude of signal spikes near each heartbeat. Finally the signal is passed through a FIR Hanning filter for smoothing.

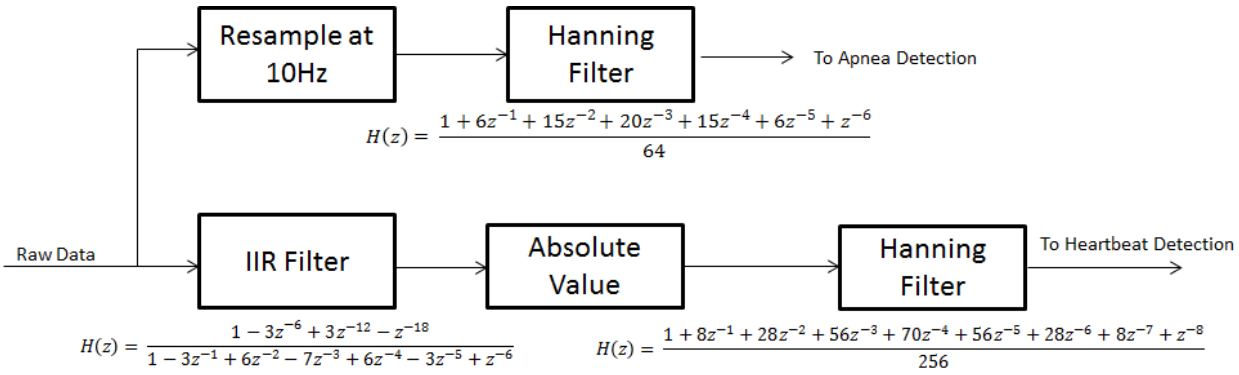

Figure 15: Digital Signal Processing Technique.

The heartbeat detection signal is compared to a hard-coded threshold; if a value is greater than the threshold it is considered a heartbeat. After a value over the threshold is detected, the heartbeat detection algorithm will ignore subsequent values over threshold for a short hard-coded refractory period so that spiking near the heartbeat peak will not be recorded as additional heartbeats.

Apnea is detected via a “walking” method, where the incoming data is constantly compared to the maximum and minimum values measured since the timer was last refreshed to zero, and in cases where they exceed the stored amount in magnitude replace them. This allows for a continuously updated wave amplitude to be calculated. When this amplitude reaches a threshold determined relative to the maximum and minimum calculation in the calibration stage, the timer is refreshed and the process repeats from that point on the wave.

Since the detection algorithm uses voltage values of individual points to detect breathing, it is susceptible to axis drift in a low amplitude signal falsely refreshing the timer, and potentially missing an apnea event, or at least delaying the alarm for longer than 15 seconds. The device compensates for this shortcoming through the use of software and analog methods. While analog components in the device do limit the ability of the signal to drift from its axis, a software solution is included because of the importance that a false negative not be produced by the device. The current detection algorithm has a weakness in that it can compare a peak from one breath to a trough of another, and see it as a successful breath. Because of this property, it becomes possible for the timer to be refreshed in instances where the signal’s axis drifts high or low over time, despite the fact that the patient is experiencing apnea. To reduce this risk, there is a timeout built into the system where no maximum or minimum value can be held longer than 4 seconds, and so slow drifting does not cause the software to falsely detect breathing. A breathing rate of 15 breaths per second corresponds to a 4 second breathing waveform, since the breathing rate of infant’s falls in the range of 30 to 60 breaths per minute; the timeout does not have the opportunity to cause the device to produce a false positive.

User Interface

Electrodes

In creating the final electrode design, four criteria were considered to ensure that the efficacy of the chosen carbon/rubber electrodes was as high as possible. These considerations were: electrode size, electrode placement, conductivity solution, and electrode to body attachment. After selecting the final specifications for each of these criteria, each variable was tested using a modification of the SAR test protocol outlined by Luo et al (1992) and detailed below.

Electrode Size

In considering electrode size, different sizes of carbon/rubber electrodes were not extensively tested as previous research clearly indicates that larger electrode size increases SAR (Luo et al 1992). Because of this fact, carbon/rubber electrodes with an approximate area of 25 cm^2 were selected for the final design. The area of these electrodes is substantially bigger than the clinical Ultra II CardioSense that were used as a control in testing. Additionally, while different carbon/rubber electrode sizes were not extensively tested, round metal discs with a much smaller area of 5.76 cm^2 were tested.

Electrode Placement

The final electrode placement was the same placement outlined by Gupta (2011). One pair of electrodes was placed below the nipple line on the left ventral side of the body and the other set on below the nipple line on the right ventral side of the body (Figure 16). This electrode placement, in addition to two other electrode placements, was tested in a previous semester (Appendix C). During that semester, it was decided that the best electrode placement would be on the right half of the body (away from the heart) with one set of electrodes below the nipple line on the ventral side of the body and another set at the same height as the first two on the dorsal side of the body. However, that selection was made in order to reduce the cardiac noise exhibited in the signal. With the reconsideration of the use of the cardiac signal as a diagnostic tool this semester, the lead placement was moved back to that outlined by Gupta (2011) in order to harness the strength of the cardiac signal for diagnostic purposes.

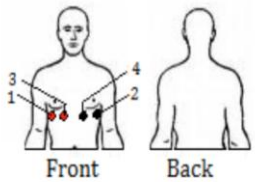

Figure 11: Diagram of lead placement on ventral side of chest cavity as proposed by Gupta (2011). Leads 1 and 2 pass carrier wave through body, leads 3 and 4 pick-up wave after it has been modulated by chest cavity.

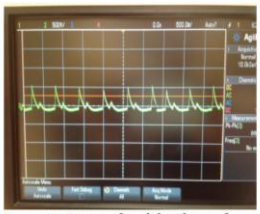

Figure 12: Picture of modulated wave from lead placement described by Gupta (2011). Lead placement shows large voltage spikes approximately once every second indicative of a cardiogenic artifact in the signal.

Figure 16: Diagram showing the electrode placement on the body. Two electrodes are placed under the nipple line on the left ventral side of the body and the remaining electrodes are placed under the nipple on the right ventral side of the body.

Additionally, over the course of the semester, the exact electrode placements were adjusted until the best signal could be achieved. Ultimately, the best placement on all three subjects tested increased the spacing between the electrode carrying the signal and the electrode reading the signal on the right side of the body but maintained the same spacing on the left side of the body.

Conductivity Solution

As another consideration to increase the efficacy of the carbon/rubber electrodes, it was the goal to design a conductivity solution that could be made from ingredients readily available anywhere in the world. The hope was that it would increase the SAR of the electrodes and could be easily remade when it ran out, thus ensuring sustainability. To achieve this end, three different conductivity solutions were created: a flour-based solution, a honey-based solution, and a glycerol-based solution.

Flour-based solution: The first of the conductivity solutions considered was designed by the Engineering World Health group at Duke University specifically for use with electrodes. The solution was a mixture of water, salt, flour, and bleach (Table 3) (www.instructables.com).

Table 3: Components of flour-based electrode solution (www.instructables.com)

Ingredient	Amount
H_2O	8 parts
NaCl	1 part
Flour	8 parts
NaClO	1 drop

Honey-based solution: The second conductivity solution was not based off of any previous design but was selected to try to incorporate adhesion into the solution to further reduce the chance of the electrodes moving. Honey was the ideal ingredient for this as it is one of the most adhesive solutions available around the world. For this solution, honey was mixed with a salt water solution.

Glycerol-based solution: The final solution considered was selected because of the gel like characteristics of glycerol. While glycerol is not a commonly available substance, it is a by-product of soap-making and can easily be obtained through mixing animal fat and lye. It was rationalized that even while not readily obtainable, it should be available worldwide. The solution was made containing four parts glycerol and one part water saturated with NaCl.

Of the three solutions, the one that was chosen for final SAR testing was the glycerol-based solution. This was because the other two solutions proved very difficult to clean off the skin and did not have the conductivity level that had been expected. The glycerol-based solution proved to be a viable method because glycerol is often used as a skin moisturizer and can be easily rubbed into the skin and because it performed well in conductivity testing.

Electrode to Body Attachment

In order to attach the carbon/rubber electrodes to the body, an elastic band that allowed for the adjustment of electrodes was designed. The band was created using a combination of ripstop and elastic. The front of the band that holds the electrodes to the body was designed using ripstop, a non-elastic fabric made out of nylon that is resistant to tearing. The back of the band was made out of elastic in order to allow the band to fit different body sizes. Velcro was attached to the carbon/rubber electrodes (Figure 17) and two lines of Velcro were attached to the inside face of the ripstop front of the band to allow for electrode adjustment. On the outside face of the ripstop as well as at the end of the elastic, a large piece of Velcro was attached that allows for the band to be tightened, fitting the size of the user. The wires for the electrodes were fed inside the band and exited the band through small holes in order to facilitate connection with the electrodes (Figure 18, Figure 19).

Figure 17: Example carbon/rubber electrode showing the Velcro placed on top of the electrode facilitating attachment to the electrode band.

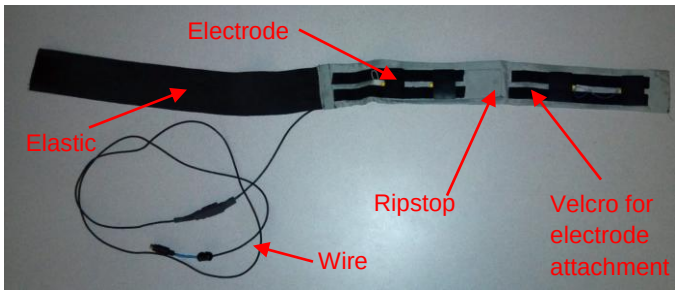

Figure 18: Electrode band prototype. Grey is the front ripstop fabric and black is the elastic band.

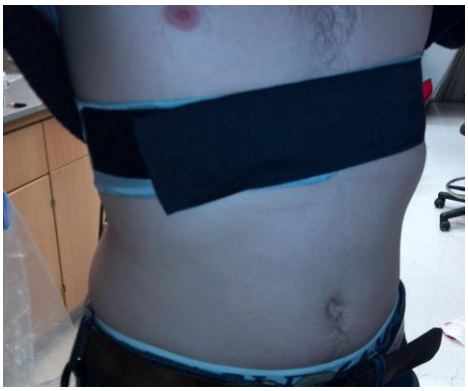

Figure 19: Electrode band prototype securely fastened on patient.

Electrode SAR Testing

As previously mentioned, the electrode placement and electrode size were not extensively tested as both had been previously tested either during previous semesters or in other literature. However, the glycerol-based conductivity solution and the electrode to body attachment were tested by analyzing the signal to artifact ratio caused by each of these design selections. SAR is a testing metric that looks to quantify the effect of motion artifacts on the desired signal, in this case respiration.

Motion artifact is one of the primary concerns to be considered when deciding on the ideal system to interface with the patient. This type of artifact arises when the electrodes acquire electromyographic (EMG) signals due to the firing of action potentials in muscles, and can also be attributed to the electrode physically translating on the skin following body movement (Kearney, 2007). One way to quantify the quality of an electrode is to determine its signal to artifact ratio, or SAR. The best performing electrodes will have a high value for SAR, meaning that the electrodes are relatively immune to EMG signals or physical translation, yet still maintain the ability to acquire the signal of interest with diagnostic quality.

The testing protocol was designed based on a modification of that presented in Luo et al (1992) and is found in its entirety in appendix D. The testing was done to look at the effects of the conductive solution and the electrode band both in isolation and in combination. The positive control used for the testing was the clinical Ultra II CardioSense electrodes and the negative control was the rubber electrodes attached to the body with tape and no conductivity solution. The following experimental conditions were setup: rubber electrode with tape and conductivity solution, rubber electrode with electrode band and no conductivity solution, and rubber electrode with electrode band and conductivity solution. Additionally, an alternative electrode type that had recently been suggested was tested, metal discs (specifically quarters), using the electrode band and tape.

Data Collection and Analysis

The data for the experiments was collected on three separate test subjects for each condition following the protocol in appendix D and was imported into Matlab for analysis. Once in Matlab, three minimum values from the respiration curve and three maximum values for the arm movement were determined using the trace tool. The average minimum voltage for respiration and the average maximum voltage for the arm movement were calculated for each subject for each test condition. The ratio of the average of the respiratory minimums to the average of artifact maximums was calculated yielding the SAR for each electrode condition for each test subject. The SAR values in each condition for each subject were averaged and the standard deviation calculated (Figure 20).

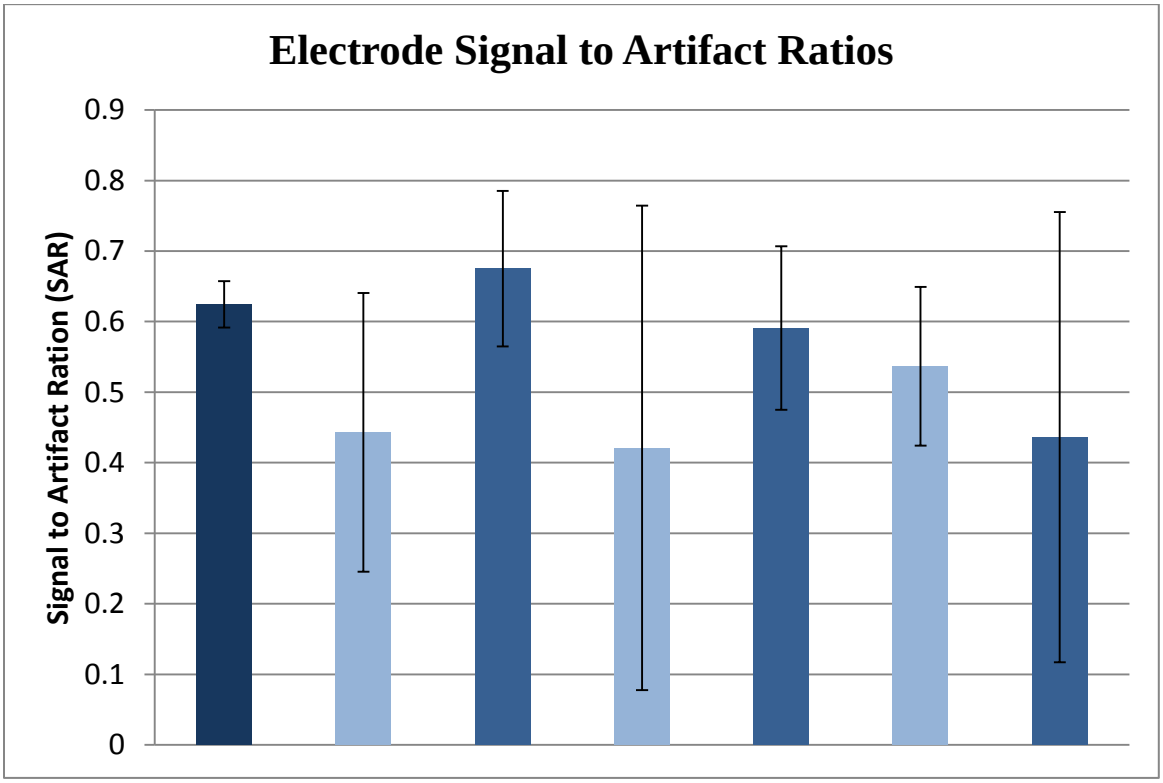

Electrode Type	Ultra II CardioSense	Rubber	Rubber	Rubber	Rubber	Metal Disc	Metal Disc
Adhesion	N/A	Tape	Band	Tape	Band	Tape	Band
Conductive Solution	N/A	No	No	Yes	Yes	No	No

Figure 20: The signal to artifact ratio of the considered electrodes. The clinical standard, Ultra II CardioSense electrodes had an average SAR of 0.624 with a standard deviation of 0.033. Rubber electrodes attached to the band with no conductive solution had an average SAR of 0.674 with a standard deviation of 0.110, and were determined to be the most viable option.

Results

Based on the results of this testing, the clinical Ultra II CardioSense electrodes had one of highest SAR value as expected, however the rubber electrodes without conductivity solution had a higher average SAR than the clinical electrodes (although it

was not statistically significant). These results indicate three things. The first is that the size of the electrodes is important as indicated in Luo et al. (1992). This conclusion is drawn from the increased SAR in the much larger rubber electrodes compared to the much smaller metal disc electrodes. While this result is likely not only due to the change in electrode size because the electrodes are made of different materials, the size of the electrodes likely did play a role. The second conclusion is that the conductivity solution reduced SAR both when the electrode band and tape were used. We hypothesize that this is because the gel was not adhesive and rather than making the electrode stick to the patient actually allowed it to move more freely and thus increased the effects of the motion artifacts. Finally, these results indicate that despite the setbacks in using carbon/rubber electrodes, using dry rubber electrodes and the electrode band should be able to yield signal to artifact ratios that are at least nearly equivalent to those obtained by the clinical electrodes.

Therefore, based on these findings, our final electrode design will take into account four factors: electrode size, electrode placement, conductivity solution, and electrode to body attachment. The electrode size used is nearly twice the area of the clinical electrodes, the electrodes will be placed under the nipple on both the left and right ventral side of the body as previously tested, no conductivity solution will be used as it has been shown to reduce SAR, and the electrodes will be held in place using a custom-build electrode band.

Device Housing

The final selection for the device housing was a Hammond black anodized aluminum box of dimensions 17.3cm x 10.8cm x 5.9cm (Figure 21). This box was selected because it meets the

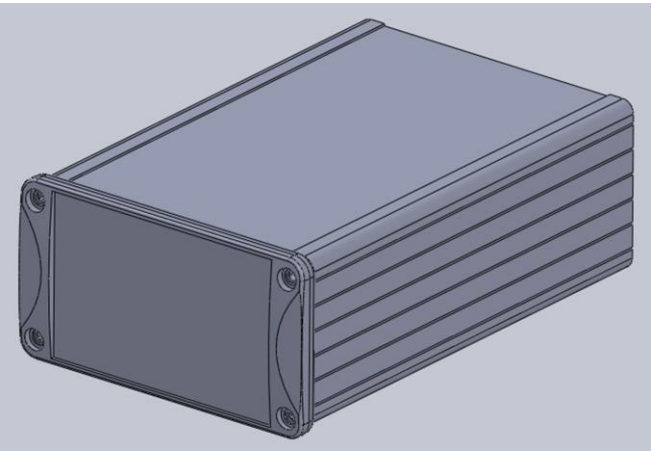

Figure 21: SolidWorks model of the cardiorespiratory monitor enclosure prior to installation of front panel (www.hammondmfg.com)

demands of the rugged conditions it may be put into. The box is completely water-proof and can bear loads of up to at least 500 lbs without deforming (www.hammondmfg.com).

The final dimensions of the box however are slightly larger than ideal dimensions of smaller than 10 cm x 10cm x 10cm, but this is necessary in order to fit the increased size of the Arduino Mega microcontroller and the wire wrapped circuit board. When the Arduino prototyping microcontroller is replaced with a smaller microcontroller and the circuit board is replaced with a printed circuit board the box design should be able to fit within the size constraints. Additionally, Hammond makes the same box design in smaller dimensions which could be used in the future to fit a smaller design.

The front panel for the prototype was made out of an acrcylic sheet cut using a laser cutter. The design for the front panel incorporates two switches for turning the device on and beginning monitoring, the electrode band connector, and three multi-colored LED signals indicating device power, cardiac events, and apnea events (Figure 22).

Finally, all of the components of the device were mounted onto an aluminum sheet that was mounted inside the box. The function of each component is detailed in the next section.

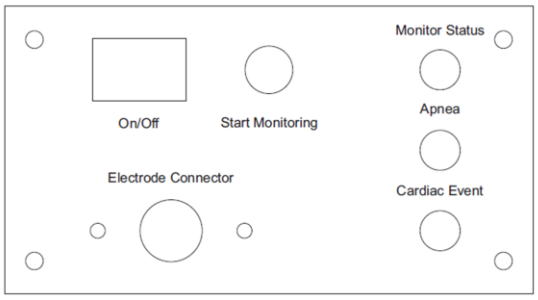

Figure 22: Laser printer design file for cardiorespiratory front panel showing all components on the front panel of the device.

External Inputs, Outputs and User Interfaces

The device enclosure was fabricated to accommodate general ease of use and to facilitate usability across a broad spectrum of social, physical, and cultural borders. With this in mind, the device's alarm scheme implements a generic three-LED visual feedback interface and a high-pitched buzzer to alert care-givers of an adverse event.

Device Power ON

The rocker switch on the front panel of the device is for turning the microcontroller ON. The microcontroller remains in an inactive state until the other toggle button is also activated.

Engage Monitor Button

Once the device is powered on, the cardiorespiratory monitor can be engaged by toggling the square push button. While the button is pushed in, the monitor will be active unless and alarm is signaled. To silence an alarm and return the cardiorespiratory monitor to an inactive state, the monitor pushbutton needs to be returned to the off (pushed out) position.

External Power

The ability to recharge the lithium polymer battery from an AC wall source is not currently supported. However, the device can be recharged using a 120V AC/5V DC converter and a USB B cable. The USB recharge port is located on the rear of the device.

Analog Waveform Output

The male BNC connector on the rear of the device is connected to the same analog signal that is fed to the analog input on the MCU. The purpose of this port is for debugging and research purposes. In the interest of reducing complexity, the future versions of this device won't provide this ability.

Electrode Input Connection

The 4-pin mini DIN connection on the front panel of the device is for connecting the device to the band of electrodes. The DIN connector is keyed to prevent improper electrical connections and possible harm to the patient.

LED Visual Feedback

The first of the three multi-color LEDs (top) on the device enclosure indicates the current power status of the device and has the following states:

- Blank: Device off, not charging
- Green: Device on, battery nominal
- Red: Low (<25%) battery
- Orange: Battery charging

The second (middle) LED is meant to visualize the current respiratory information being received by the device and is only active when the device is monitoring a patient. The green light pulses and fades with the inhalation and exhalation of the patient and turns solid red when the device has detected an apneic event is occurring.

The third (bottom) LED is meant to visualize the current ECG signal that is being received by the device and is only active when the device is monitoring a patient. The green light blinks every time a QRS complex is detected and turns solid red when a critically low heart rate is measured.

Budget

Throughout the design process, the cost of various design options weighed heavily on decisions, because of the nature of the problem that is being addressed. The target cost of the end product is $30, which is an estimate taking quantity of scale into account. The materials used to build the prototype designed this semester cost $90.97 (Table 4), not including to the labor to assemble it. At this stage, the prototype relies on an Arduino Mega 2560 microcontroller to run the detection algorithms on the incoming data, as well as to monitor the battery power. The next iteration of the device will utilize a much less expensive microcontroller, as well as a printed circuit board, rather than a wire wrapped prototype.

Item	Unit Cost	Quantity	Extended Cost

22 uf Cap	$0.19	1	$0.19
2.7 k Res	$0.07	1	$0.07
560 Res	$0.13	4	$0.52
24 k Res	$0.13	1	$0.13
47 pF Cap	$0.19	1	$0.19
15 k Res	$0.22	1	$0.22
10 uF Cap	$0.37	1	$0.37
10 nF Cap	$0.12	7	$0.84
100 nF Cap	$0.12	1	$0.12
25 k Res	$0.13	4	$0.52
250 k Res	$0.19	4	$0.76
LT 1920 Instrumentation Amp	$5.50	1	$5.50
TLV274 Operational Amp	$1.42	2	$2.84
Bat 46 Shocktey Diode	$0.25	2	$0.50
LiPo Powercell	$19.95	1	$19.95
Headers, Perf-board, Wires	$5.00	1	$5.00
Circuit Housing	$33.25	1	$33.25
Electrode Band	$20.00	1	$20.00
Total Cost			**$90.97**

Table 4: Bill of materials that were required to build the current prototype.

Safety and Compliance

In order for this infant respiratory monitor to be effective from an Engineering World Health standpoint, it must harbor the necessary approvals from regulatory agencies, deeming it safe for patient use. After assessing the rate of infant mortality in developing countries throughout the world, and taking into account current partnerships, it was decided that this device will first be implemented in Ethiopia.

The Ministry of Health is responsible for the accessibility of quality health service to all citizens throughout Ethiopia, and more specifically, the *Food, Medicine and Health Care Administration and Control Authority of Ethiopia (FMHACA)* provides the checks and balances between different directorates. *FMHACA* references many of the same international standards as the *US Food and Drug Administration (FDA)*, and the *Medical Device Directive (MDD)*, but is still not as acutely regulated as the aforementioned. Documentation for device design and testing is more explicitly defined by the *FDA* and

MDD, so in order to ensure that the device is designed with patient safety as the highest priority, the device will be designed according to the guidelines laid out by the *FDA*.

The *FDA* identifies an apnea monitor as:

"An apnea monitor is a complete system intended to alarm primarily upon the cessation of breathing timed from the last detected breath. The apnea monitor also includes indirect methods of apnea detection such as monitoring of heart rate and other physiological parameters linked to the presence of absence of adequate respiration."

(FDA Code of Federal Regulations, 2002)

Apnea monitors are *Class II* medical devices according the *FDA*, and *Class IIb* medical devices by the *MDD's* standards, meaning that they pose "medium risk" to patient safety. *Class II* devices encapsulate a wide variety of devices, ranging from apnea monitors to surgical lasers, and because of this, all devices of this classification are accompanied by a special control document. For apnea monitors, this document highlights the risks associated with using the device, which can then be decomposed into design requirements that must be included to minimize the risk and therefore comply with standards set by the *FDA*. It also includes relevant material for testing and validation to be submitted with a 510(k) premarket notification. 510(k) premarket notifications are required of medical devices that have already been approved for market; therefore in order to gain approval, thorough testing will be required to prove that the device is substantially equivalent to those already on the market. Figure 15 below outlines a general overview of the possible routes that can be taken in pursuit of device approval.

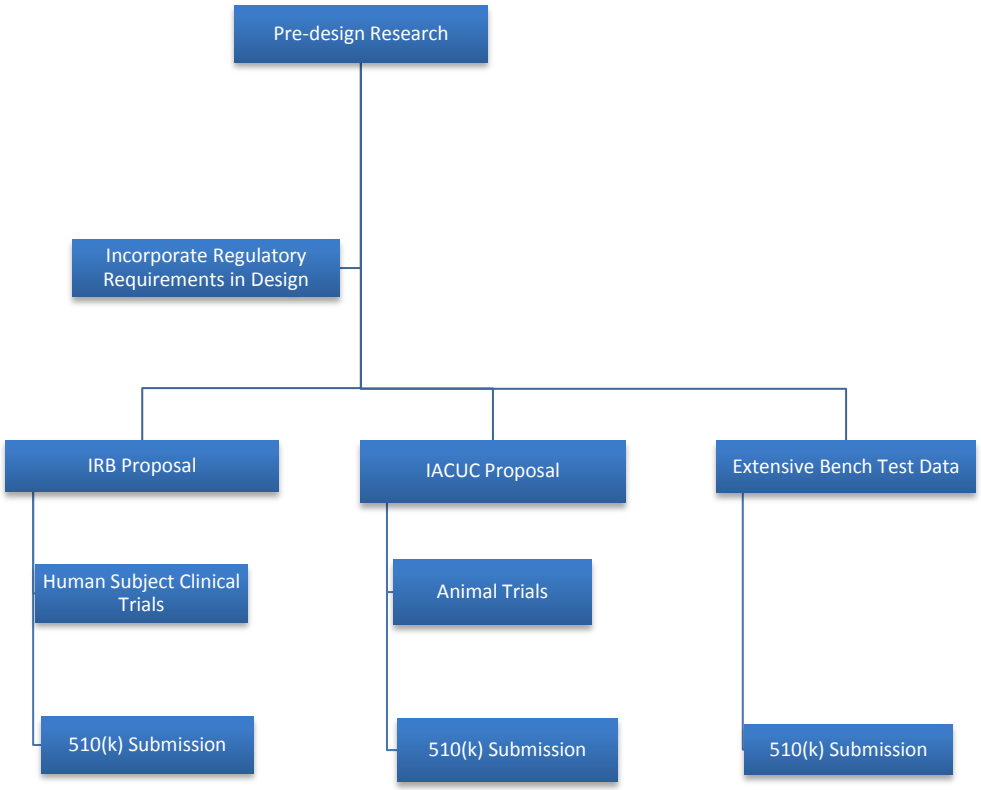

Figure 23: Flowchart illustrating possible routes to 510(k) premarket submission.

The special control document for apnea monitors identifies the following risks to health associated with apnea monitors: Inadequate alarms, electrical shock, electromagnetic interference, inaccurate detection, and tissue reactivity. These risks can be managed with the integration of necessary electrical components, proper software validation through scenario based bench testing, and the design of an electrode system using biocompatible materials where patient contact occurs over long durations of time. In reference to figure 23, the pre-design research includes risk assessment included in *FDA's* control document.

As the project progresses, the team will continue to break down the risks highlighted by the *FDA*, and minimize them through testing of leakage currents, proper electrode selection, and scenario based bench testing to validate the software algorithms. When sufficient proof of concept data has been collected, it will be decided whether clinical trials, animal trials, or thorough bench testing will be required for submission of a 510(k) premarket notification.

Future Work

The ultimate purpose of this device is to be implemented in developing countries. In order to reach this point there is still work to be done. Throughout the semester, the team will maintain communication with contacts in the industry to ensure that the finished product may be implemented quickly when the time comes. The team will also need to complete rigorous bench testing on the final product to be eligible for a 510(k) premarket notification. The major development work to be accomplished for the product consists of two categories: software and hardware.

Hardware

The prototype fabricated this semester used an arduino device to allow easy access to the pins of the flat package microcontroller. In future devices, a printed circuit board will include the analog components of the device, as well as the microcontroller. A printed board will allow for larger scale production, as well as shorter fabrication time of the final product. Additionally, telemedicine components will be included. Necessary components for a telemedicine device include memory external to the mcu, as well as a SPI or I2C interface to communicate with external devices. To communicate serially from the mcu, a max 232 or similar component will be needed to correct the voltage between the devices.

Software

The software utilized now is an improvement over the prior semesters' because it includes a better detection algorithm, and has a "smarter" calibration method that allows it to ignore outlying signals during startup. It also has a far more comprehensive signal processing method built into it. However, the calibration of the device can be further improved by including a calibration stage for the QRS detection threshold, and by converting the logic of the device to mimic a finite state machine, which will produce a more intuitive logic structure and help optimize the code to be less costly in terms of time and memory operations, and by extension, power. This would in turn allow the device to use a chip with fewer features, and bring down the overall cost of the product.

References

3B Scientific W53112SB Black Round Carbon Rubber Electrodes, 2" Diameter. 2012. Amazon.com Online Store. http://www.amazon.com/3B-Scientific-W53112SB-Electrodes-Diameter/dp/B005F5O8XK/ref=sr_1_3?ie=UTF8&qid=1351043973&sr=8-3&keywords=rubber+electrode.

3M Red Dot Multi-Purpose Monitoring Electrode, Foam, 50/bg. 2012. Amazon.com Online Store. http://www.amazon.com/Red-Dot-Multi-Purpose-Monitoring-Electrode/dp/B002C2M90I/ref=sr_1_1?ie=UTF8&qid=1351044031&sr=8-1&keywords=3M+red+dot

Anglecare Monitors Inc. – Movement and Sound Monitor. Retrieved 10/22/12 from http://www.angelcare- monitor.com/International/en/products/angelcare-monitor-AC201

Atmel online store. (store.atmel.com)

ATmega640/V, ATmega1280/V, ATmega1281/V, ATmega2560/V, ATmega2561/V Data Sheet. Atmel Corporation.

Been, Y. S., Khan, J. N., & Hui, D. C. (2007, May 24). Designing medical devices for isolation and safety | EDN. EDN. Retrieved October 22, 2012, from http://www.edn.com/design/medical/4314949/Designing-medical-devices-for-isolation-and-safety

Berrington, J.E., Hearn, R.I., Bythell, M., Wright, C.,Embleton, N.D. 2012. Deaths in Preterm Infants: Changing Pathology Over 2 Decades. The Journal of Pediatrics 160:49-53.

Chen, S., Ravallion, M. 2008. The developing world is poorer than we thought, but no less successful in the fight against poverty. World Bank, August 2008.

Class II Special Controls Guidance Document: Apnea Monitors; Guidance for Industry and FDA [Online]. (2002). Available FTP: http://www.fda.gov/MedicalDevices/DeviceRegulationandGuidance/GuidanceDocuments/ucm072846.htm

Ersdal, H.L., Mduma, E., Svensen, E., Perlamn, J. 2011. Birth Asphyxia: A Major Cause of Early Neonatal Mortality in a Tanzanian Rural Hospital. Pediatrics 2011:3134-3141.

FDA Code of Federal Regulations Title 21, Part 868 -- Anesthesiology Devices, 2002.

Grenvik et al. Impedance Pneumography: Comparison between chest impedance changes and respiratory volumes in II healthy Volunteers. Chest 1972: 62:439-443.

Gupta, A.K. 2011. Respiration Rate Measurement Based on Impedance Pneumography. Texas Instruments Application Report SBAA181.

Hisense Ltd. Babysense. Retrieved 10/22/12 from http://www.hisense.co.il/catalog.php?id=16

Infantrust Parenting Solutions Ltd. - Respisense. Retrieved 10/22/12 from http://www.respisense.com/en/index.php

Kearney, K., et al. (2007, August). Quantification of Motion Artifact in ECG Electrode Design. Sensor Technology & Devices Ltd., 4 Heron Road, Belfast, UK. [Online]. Available: http://www.ncbi.nlm.nih.gov/pubmed/18002260

Lawn, J.E., Cousens, S., Zupan, J. 2005. 4 million neonatal deaths: When? Where? Why? Lancet 365:891-900.

Luo, S., Afonso, V.X., Webster, J.G., Tompkins, W.J. 1992. The Electrode System in Impedance-Based Ventilation Measurement. IEEE Transactions on Biomedical Engineering 39(11):1130-1141.

Marcus, C.L. 2001. Sleep-disordered Breathing in Children. American Journal of Respiratory and Critical Care Medicine 164:16-30.

Norman et al. Detection of Respiratory Events during NPSG: Nasal Cannula/Pressure Sensor versus Thermistor. Sleep 20 (12): 1175-1184.

Pizzuti, G., S. Cifaldi, and G. Nolfe. "Digital Sampling Rate and ECG Analysis." *Journal of Biomedical Engineering* 7.3 (1985): 247-50. *Pubmed.gov*. 2012.

Rocker, J.A., Israel, J. 2012. Pediatric Apnea. Medscape Online Refrerence: http://emedicine.medscape.com/article/800032-overview.

Standards and Guidlines Compiled at DACA. (n.d.). Ethiopian Drug Administration and Control Authority Home Page. Retrieved October 23, 2012, from http://www.fmhaca.gov.et/standardsandguidlines.html

SUDC Home Monitoring for SUDC Siblings. Retrieved 10/22/12 at http://www.sudc.org/Portals/0/medical/HomeMonitoringForSUDCSiblings.pdf

Tompkins, W. J., (1993). *Biomedical Digital Signal Processing*. 3rd ed. Boston: Prentice Hall.

UNICEF. 2012. Levels & Trends in Child Mortality, Report 2012. The Unite4d Nations Children's Fund.

Mayotte, M.J., Webster, J.G., Tompkins, W.J. 1994. A comparison of electrodes for potential use in paediatric/infant apnoea monitoring. Physiological Measurements 15:459-467.

Appendix A: Product Design Specifications

Engineering World Health: Infant Respiratory Monitor
Preliminary Product Design Specifications
Caleb Durante, Drew Birrenkott, Don Weier, Michael Nonte, Bradley Wendorff

Function:
The monitor shall function as an early warning and detection system of infant central apnea in developing countries by providing a reliable detection mechanism that alerts nearby caretakers of an adverse event. Using captured respiratory and ECG data, the monitor will trigger its alarm after breathing ceases for more than 20 seconds, or if the average heart rate falls below 60 beats per minute. This will allow the caretaker a greater amount of time to determine the proper course of action to resuscitate the infant.

Client Requirements:
1) The monitor must cost under $30.
2) The monitor must be reliable and consistently alert caretakers when breathing has stopped for more than 20 seconds or if the average heart rate ever falls below 60 beats per minute.
3) The monitor must be easy to operate with minimal training.
4) The monitor must be tamper-proof with no user serviceable parts (excluding battery)
5) The monitor should be suitable for use in newly industrialized and developing nations.

Physical and Operational Characteristics:

a. *Performance Requirements:*

- The monitor must be capable of monitoring an infant's breathing pattern and alerting nearby caretakers if there is a 20 second or more cessation in breathing.
- The monitor must be capable of monitoring an infant's heart rate and alert nearby caretakers if there is a drop in heart rate below 60 beats per minute.

b. *Safety:*

- The monitor cannot interfere with healthy bioelectrical electrical signals in the infant or present a shock risk to an operator.
- Any external wiring must not present a strangulation risk.
- There should be no small, easily breakable parts that can present a choking hazard.
- The alarm shall not be above levels which damage the infant's hearing ability
- The monitor must meet all regulatory demands outlined by government or other agencies.

c. *Accuracy and Reliability:*

- The monitor must have reliable accuracy, and cannot allow for a false negative in the monitor.
- The design must minimize the occurrence of false positives to maintain user confidence in the monitor

d. *Life in Service:*

- Excluding the monitor's battery and lead system, the monitor shall function for at least 5-10 years.
- The monitor must be able to withstand reasonable wear due to use.
- The monitor must be designed to minimize the risk of broken parts.

e. *Shelf Life:*

- Excluding the monitor's battery and lead system, the monitor shall function for at least 5-10 years regardless of usage frequency.
- The monitor will require batteries that should be easily replaced.

f. *Operating Environment:*

- The monitor should be designed to function in a mobile hospital setting
- The monitor shall be able to tolerate temperature ranges of 0-41 degrees C
- The monitor enclosure shall prevent the buildup of ambient particulate on the inner electronic components
- The monitor enclosure shall prevent the encroachment of moisture within its housing

g. *Ergonomics:*

- The monitor should not interfere with comfortable sleep.
- The monitor electrode system shall be designed to ensure consistent placement location on the infant's body

h. *Size:*

- The monitor should have a maximum size of 10x10x5 cm.
- The monitor's electrode band shall be designed according to anthropometric data from infants under 1 year of age

i. *Power Source:*

- The monitor will be battery-powered and should maximize power efficiency
- The monitor shall operate continuously for 24 hours on a single fully-charged battery
- The batteries shall be rechargeable, allowing for pairs of batteries to be cycled for use in the same monitor without disruption of daily monitor usage

j. *Weight:*

- The monitor must be lightweight, not exceeding 1.0 kg but weigh more than 200g

k. *Materials:*

- The monitor shall consist of a printed-circuit board including both passive elements and active integrated circuits, as well as a microprocessor.
- The electronic components will reside within a plastic enclosure with holes machined for external connections to electrodes
- The monitor housing will contain one buzzer/speaker
- The housing must be sterilizable

l. *Aesthetics, Appearance, and Finish:*

- The monitor appearance should align with other devices found in a hospital setting
- The monitor's controls shall be easily understood and operated by individuals from all cultures, races, and dialects

m. *Product Characteristics:*

- Quantity: Two
- Target Product Cost: $10 - $30

n. Miscellaneous:

Standard and Specification:

- The monitor must comply with HIPPA, AAMI , and patient disclosure standards

Patient-Related Concerns:

- Device components in contact with the infant must receive sterilization between uses.
- Must not pose risk of shock or infant entanglement.

Competition:

- Devices on the market include the products made by Babysense, Respisense, CloudMonitor, AngleCare, and Snuza

Customer: **Engineering World Health or Similar NGO**

Appendix B: Atmel 2560 Specification Sheet

Features

- High Performance, Low Power Atmel® AVR® 8-Bit Microcontroller
- Advanced RISC Architecture
  - 135 Powerful Instructions – Most Single Clock Cycle Execution
  - 32 x 8 General Purpose Working Registers
  - Fully Static Operation
  - Up to 16 MIPS Throughput at 16MHz
  - On-Chip 2-cycle Multiplier
- High Endurance Non-volatile Memory Segments
  - 64K/128K/256KBytes of In-System Self-Programmable Flash
  - 4Kbytes EEPROM
  - 8Kbytes Internal SRAM
  - Write/Erase Cycles:10,000 Flash/100,000 EEPROM
  - Data retention: 20 years at 85°C/ 100 years at 25°C
  - Optional Boot Code Section with Independent Lock Bits
    - In-System Programming by On-chip Boot Program
    - True Read-While-Write Operation
  - Programming Lock for Software Security
    - Endurance: Up to 64Kbytes Optional External Memory Space
- Atmel® QTouch® library support
  - Capacitive touch buttons, sliders and wheels
  - QTouch and QMatrix® acquisition
  - Up to 64 sense channels
- JTAG (IEEE std. 1149.1 compliant) Interface
  - Boundary-scan Capabilities According to the JTAG Standard
  - Extensive On-chip Debug Support
  - Programming of Flash, EEPROM, Fuses, and Lock Bits through the JTAG Interface
- Peripheral Features
  - Two 8-bit Timer/Counters with Separate Prescaler and Compare Mode
  - Four 16-bit Timer/Counter with Separate Prescaler, Compare- and Capture Mode
  - Real Time Counter with Separate Oscillator
  - Four 8-bit PWM Channels
  - Six/Twelve PWM Channels with Programmable Resolution from 2 to 16 Bits (ATmega1281/2561, ATmega640/1280/2560)
  - Output Compare Modulator
  - 8/16-channel, 10-bit ADC (ATmega1281/2561, ATmega640/1280/2560)
  - Two/Four Programmable Serial USART (ATmega1281/2561, ATmega640/1280/2560)
  - Master/Slave SPI Serial Interface
  - Byte Oriented 2-wire Serial Interface
  - Programmable Watchdog Timer with Separate On-chip Oscillator
  - On-chip Analog Comparator
  - Interrupt and Wake-up on Pin Change
- Special Microcontroller Features
  - Power-on Reset and Programmable Brown-out Detection
  - Internal Calibrated Oscillator
  - External and Internal Interrupt Sources
  - Six Sleep Modes: Idle, ADC Noise Reduction, Power-save, Power-down, Standby, and Extended Standby
- I/O and Packages
  - 54/86 Programmable I/O Lines (ATmega1281/2561, ATmega640/1280/2560)
  - 64-pad QFN/MLF, 64-lead TQFP (ATmega1281/2561)
  - 100-lead TQFP, 100-ball CBGA (ATmega640/1280/2560)
  - RoHS/Fully Green
- Temperature Range:
  - -40°C to 85°C Industrial
- Ultra-Low Power Consumption
  - Active Mode: 1MHz, 1.8V: 500µA
  - Power-down Mode: 0.1µA at 1.8V
- Speed Grade:
  - ATmega640V/ATmega1280V/ATmega1281V:
    - 0 - 4MHz @ 1.8V - 5.5V, 0 - 8MHz @ 2.7V - 5.5V
  - ATmega2560V/ATmega2561V:
    - 0 - 2MHz @ 1.8V - 5.5V, 0 - 8MHz @ 2.7V - 5.5V
  - ATmega640/ATmega1280/ATmega1281:
    - 0 - 8MHz @ 2.7V - 5.5V, 0 - 16MHz @ 4.5V - 5.5V
  - ATmega2560/ATmega2561:
    - 0 - 16MHz @ 4.5V - 5.5V

8-bit Atmel Microcontroller with 64K/128K/256K Bytes In-System Programmable Flash

ATmega640/V
ATmega1280/V
ATmega1281/V
ATmega2560/V
ATmega2561/V

2549P–AVR–10/2012

Appendix C: Lead Placement Testing (12/12/2011)

After completing construction of the final design circuit, human testing on an adult male test subject was conducted to determine proper lead placement to achieve the greatest peak to peak voltage change upon inhalation. Initial lead placement was based on the design of Gupta (2011) with two leads on both halves of the ventral side of the chest (Figure 1B). With this lead configuration the carrier signal is transmitted between the lateral pair of leads and the modulated wave is detected on the medial pair of leads (Figure 1B). Results from this lead configuration returned a large voltage spike approximately once every second, indicating a cardiogenic artifact that was greater than the peak to peak due to respiration (Figure 2B).

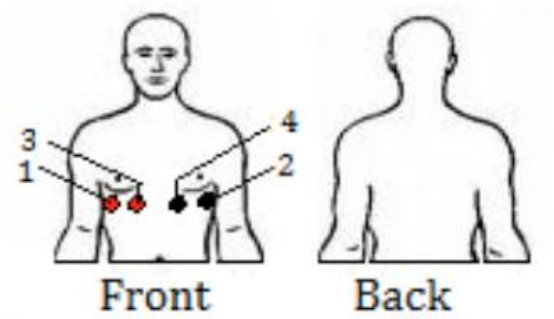

Figure 1B: Diagram of lead placement on ventral side of chest cavity as proposed by Gupta (2011). Leads 1 and 2 pass carrier wave through body, leads 3 and 4 pick-up wave after it has been modulated by chest cavity.

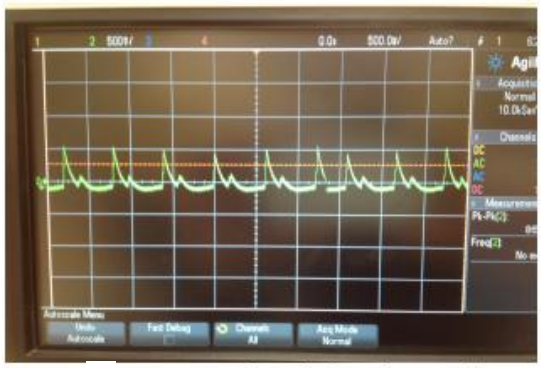

Figure 2B: Picture of modulated wave from lead placement described by Gupta (2011). Lead placement shows large voltage spikes approximately once every second indicative of a cardiogenic artifact in the signal.

In order to reduce the cardiac artifact and amplify the voltage change due to respiration, two additional lead placements were tried. One lead placement was identical to the initial lead placement except that the leads were moved above the nipple line in an attempt to reduce the effect of the heart's electric signal (Figure 3B). This lead configuration led to a decreased heart artifact but was subject to the electrical signal created by the pectoral muscles upon flexing and relaxing. The third lead placement incorporated leads below the nipple line on the right ventral and dorsal sides of the chest cavity with one carrier lead and one lead reading the modulated wave on both sides (Figure 4B). The lateral leads were for the carrier wave and the medial leads were for detecting the modulated wave (Figure 5B). This lead placement produced a peak to peak voltage of 250 mV during tidal breathing, the greatest peak to peak voltage change of the three lead placements, and also had the smallest cardiogenic artifact (Figure 5B).

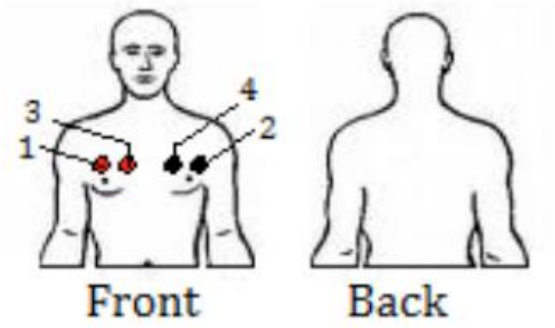

Figure 3B: Diagram of lead placement above the nipple line on the pectoral muscles. Leads 1 and 2 pass carrier wave through body, leads 3 and 4 pick-up wave after it has been modulated by chest cavity.

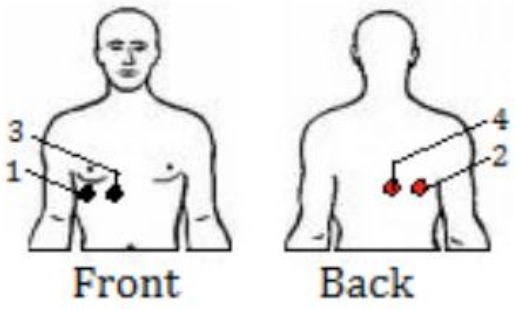

Figure 4B: Diagram of lead placement on the right ventral and dorsal sides of the body. Leads 1 and 2 pass carrier wave through body, leads 3 and 4 pick-up wave after it has been modulated by chest cavity.

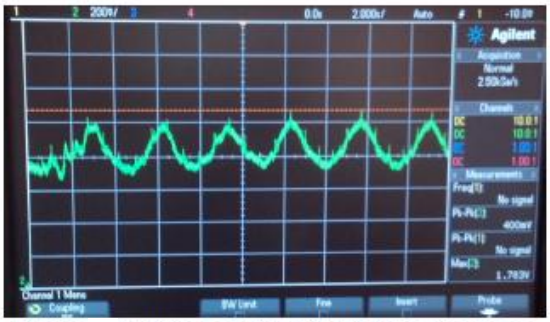

Figure 5B: Picture of modulated wave from third lead placement option. Lead placement shows rhythmic voltage change on respiration. Small spikes in voltage can be seen on waveform indicating remnants of cardiogenic artifact.

Appendix D: Electrode Test Protocol

Without Band

The testing of electrodes without the band is conducted on the carbon rubber electrodes both with and without conductive solution, the metal discs, and the clinical electrodes.

1. Lay subject down on a table so that all muscles are relaxed. The carrier signal supplying electrode and ground electrode are positioned on opposing sides of the thorax, while the voltage measuring electrodes are positioned ~5 cm (Pending patient anatomy, one electrode is positioned over the apex of the heart) medial to the carrier current electrodes.
2. When the positions are set, the electrodes should be securely attached to the patient's body with electrical tape, making sure not to allow any tape fold over between the electrode and the skin.
3. The carrier signal is passed through the subject, and the output from the circuit is displayed on the oscilloscope for data collection.
4. The subject continues relaxed, comfortable breathing for one minute, or until a series of five quality respirations can be saved.
5. After the data has been saved for the relaxed breathing, the patient remains on their back, and should then inhale, and exhale until they reach residual volume in their lungs.
6. The subject should hold their breath until the signal on the oscilloscope flat-lines, and continues holding their breath throughout the data collection.
7. The subject moves their extended arms in a motion with so that the hand moves from hip to full abduction (away from the body).
8. Continue the arm motion until at least five peaks and troughs are detected.
9. The same patient undergoes successive trials with each electrode to ensure placement is consistent.
    a. For the rubber electrodes, the conductive solution test should completed after the data for the dry rubber electrodes has been gathered.
    b. To apply the gel solution remove a strip of tape, then add 2-3 drops of solution between the electrode and skin. Re-apply the tape, and the data is collected using the same procedure as previously defined.

With Band

1. Fasten the electrode of interest to the electrode band so that they are positioned in the same locations as was previously used for the tests without the band.
2. When the positions are set, the subject should lay down. The carrier signal is passed through the subject, and the output from the circuit is displayed on the oscilloscope for data collection.
3. The subject continues relaxed, comfortable breathing for at least one minute or until a series of five quality respirations can be saved.
4. After the data has been saved for the relaxed breathing, the patient remains on their back, and should then inhale, and exhale until they reach residual volume in their lungs.

5. The subject should hold their breath until the signal on the oscilloscope flat-lines, and continues holding their breath throughout the data collection.
6. The subject moves their extended arms in a motion with so that the hand moves from hip to full abduction (away from the body).
7. Continue the arm motion until at least five peaks and troughs are detected.
8. The same patient undergoes successive trials with each electrode to ensure placement is consistent.
    a. For the rubber electrodes, the conductive solution test should be completed after the data for the dry rubber electrodes has been gathered.
    b. To apply the conductive solution remove a strip of tape, then add 2-3 drops of solution between the electrode and skin. Re-apply the tape, and the data is collected using the same procedure as previously defined.

Appendix E: C Code

```
/*****************************************************
Project : Infant Respiratory and Cardiac Monitor
Date    : 12/9/2012
Author  : Mike Nonte, Don Weier
Chip type               : ATmega2560
Program type            : Application
AVR Core Clock frequency: 8.000000 MHz
Memory model            : Small
External RAM size       : 0
Data Stack size         : 2048
*****************************************************/
#include <avr/interrupt.h>
#include <avr/io.h>
#include <stdio.h>
#include <stdint.h>
#include <math.h>
#include <util/delay.h>
#include <stdio.h>

//Disable/Enable masks for timer ISRs
#define ENABLE_SAMP1 0x02;
#define DISABLE_SAMP1 0xF8;
#define ENABLE_HL3 0x04;
#define DISABLE_HL3 0xF8;
#define ENABLE_ALM4 0x05;
#define DISABLE_ALM4 0xF8;
#define ENABLE_WAIT5 0x02;
#define DISABLE_WAIT5 0xFD;
#define SAMP1_TOG TCCR1B;
#define HL3_TOG TCCR3B;
#define ALM4_TOG TCCR4B;
#define WAIT5_TOG TCCR5B;

//Filter Coefficients
uint16_t hanningNumCo_b[]= {1, 6, 15, 20, 15, 6, 1};
uint16_t hanningDenCo_b[] = {64};
uint16_t hanningNumCo_e[] = {1,8,28,56,70,56,28,8,1};
uint16_t hanningDenCo_e[] = {256};
uint16_t IIRfiltNumCo[] = {1,-3,3,-1};
uint16_t IIRfiltDenCo[] = {1,-3,6,-7,6,-3,1};

//Storage arrays for feedforward and feedback filter terms
volatile uint16_t BREATHFILTERSTORAGE[7];
volatile uint16_t IIROUTPUTSTORAGE[6];
volatile uint16_t ECGFILTERSTORAGE[9];

//Storage arrays for current "stream" of data
volatile uint16_t BREATHDATA[20];
volatile uint16_t RAWDATA[19];
volatile uint16_t ECGDATA[20];

//Calibration variables
volatile uint16_t initialMAX[8];
volatile uint16_t initialMIN[8];
volatile uint16_t initializeinc=0;
volatile uint16_t datagrab[5];//holds current input value during setup of breathing
threshold
volatile uint16_t deltaave; //used to store a benchmark for breathing to compare to
volatile uint16_t resample = 0;//marks which data should be used for breath detection
volatile uint16_t alarmcount = 0;
```

```
volatile uint16_t MinTik = 0; //tracks time since currentmin was set
volatile uint16_t MaxTik = 0;//tracks current max

//Alarm State variables
volatile uint16_t countover5 = 0; //uses to shortcut to alarm if no HB detected for 5
seconds
volatile uint16_t breaththresh = 0; //set to true for 2s after an acceptable breath is
detected
volatile uint16_t threshcount;// used to track breaththresh = 1 for 2s then toggle it
off
volatile uint16_t countover15 = 0;//tracks if HR is too slow over time

//Respiratory/Cardiac metrics
volatile uint16_t HBcount = 0; //this will count between detected heartbeats to
determine which bools should be set to control the ALARM trigger
volatile uint16_t currentmax=1;
volatile uint16_t currentmin=1023;//these will store the current max/min since last
breath threshold was met
volatile uint16_t deltacurrent;

//Function Declarations
uint16_t adc_read(uint8_t ch);
volatile uint16_t BREATHFILTER();
volatile uint16_t ECGFILTER();
static int uart_putchar(char c, FILE *stream);
static FILE mystdout = FDEV_SETUP_STREAM(uart_putchar, NULL, _FDEV_SETUP_WRITE);
//Define stream to use when calling stdio.h functions
void wait(uint16_t ms);
void checkALARM();

void main(void){
    // Crystal Oscillator division factor: 1
    #pragma optsize-
    CLKPR=0x80;
    CLKPR=0x00;
    #ifdef _OPTIMIZE_SIZE_
    #pragma optsize+
    #endif
    cli(); //Disable Global Interrupts

    // Input/Output Ports initialization
    // Port A initialization
    // Func7=In Func6=In Func5=In Func4=In Func3=In Func2=In Func1=In Func0=In
    // State7=T State6=T State5=T State4=T State3=T State2=T State1=T State0=T
    PORTA=0x00;
    DDRA=0x00;

    // Port B initialization
    // Func7=In Func6=In Func5=Out Func4=Out Func3=Out Func2=Out Func1=Out Func0=Out
    // State7=T State6=T State5=0 State4=0 State3=0 State2=0 State1=0 State0=0
    PORTB=0x00;
    DDRB=0x3F;

    // Port C initialization
    // Func7=Out Func6=Out Func5=Out Func4=Out Func3=Out Func2=Out Func1=Out Func0=Out
    // State7=0 State6=0 State5=0 State4=0 State3=0 State2=0 State1=0 State0=0
    PORTC=0x00;
    DDRC=0xFF;


    // Port D initialization
    // Func7=In Func6=In Func5=In Func4=In Func3=In Func2=In Func1=In Func0=In
    // State7=T State6=T State5=T State4=T State3=T State2=T State1=T State0=T
```

```
PORTD=0x00;
DDRD=0x00;

// Port E initialization
// Func7=In Func6=In Func5=In Func4=In Func3=In Func2=In Func1=In Func0=In
// State7=T State6=T State5=T State4=T State3=T State2=T State1=T State0=T
PORTE=0x00;
DDRE=0x00;

// Port F initialization
// Func7=In Func6=In Func5=In Func4=In Func3=In Func2=In Func1=In Func0=In
// State7=T State6=T State5=T State4=T State3=T State2=T State1=T State0=T
PORTF=0x00;
DDRF=0x00;

// Port G initialization
// Func5=In Func4=In Func3=In Func2=In Func1=In Func0=In
// State5=T State4=T State3=T State2=T State1=T State0=T
PORTG=0x00;
DDRG=0x00;

// Port H initialization
// Func7=In Func6=In Func5=In Func4=In Func3=In Func2=In Func1=In Func0=In
// State7=T State6=T State5=T State4=T State3=T State2=T State1=T State0=T
PORTH=0x00;
DDRH=0x00;

// Port J initialization
// Func7=In Func6=In Func5=In Func4=In Func3=In Func2=In Func1=In Func0=In
// State7=T State6=T State5=T State4=T State3=T State2=T State1=T State0=T
PORTJ=0x00;
DDRJ=0xFF;

// Port K initialization
// Func7=In Func6=In Func5=In Func4=In Func3=In Func2=In Func1=In Func0=In
// State7=T State6=T State5=T State4=T State3=T State2=T State1=T State0=T
PORTK=0x00;
DDRK=0x00;


// Port L initialization
// Func7=In Func6=In Func5=In Func4=In Func3=In Func2=In Func1=In Func0=In
// State7=T State6=T State5=T State4=T State3=T State2=T State1=T State0=T
PORTL=0x00;
DDRL=0x00;

// Timer/Counter 0 initialization
// Clock source: System Clock
// Clock value: Timer 0 Stopped
// Mode: Normal top=0xFF
// OC0A output: Disconnected
// OC0B output: Disconnected
TCCR0A=0x00;
TCCR0B=0x00;
TCNT0=0x00;
OCR0A=0x00;
OCR0B=0x00;

// Timer/Counter 1 initialization
// Clock source: System Clock
// Clock value: 8000.000 kHz
// Mode: CTC top=OCR1A
// OC1A output: Discon.
```

```
// OC1B output: Discon.
// OC1C output: Discon.
// Noise Canceler: Off
// Input Capture on Falling Edge
// Timer1 Overflow Interrupt: On
// Input Capture Interrupt: Off
// Compare A Match Interrupt: On
// Compare B Match Interrupt: Off
// Compare C Match Interrupt: Off
TCCR1A=0x00;
TCCR1B=0x08;
TCNT1H=0x00;
TCNT1L=0x00;
ICR1H=0x00;
ICR1L=0x00;
OCR1AH=0x4E;
OCR1AL=0x1C;
OCR1BH=0x00;
OCR1BL=0x00;
OCR1CH=0x00;
OCR1CL=0x00;

// Timer/Counter 2 initialization
// Clock source: System Clock
// Clock value: Timer2 Stopped
// Mode: Normal top=0xFF
// OC2A output: Disconnected
// OC2B output: Disconnected
ASSR=0x00;
TCCR2A=0x00;
TCCR2B=0x00;
TCNT2=0x00;
OCR2A=0x00;
OCR2B=0x00;

// Timer/Counter 3 initialization
// Clock source: System Clock
// Clock value: 125.000 kHz
// Mode: CTC top=OCR3A
// OC3A output: Discon.
// OC3B output: Discon.
// OC3C output: Discon.
// Noise Canceler: Off
// Input Capture on Falling Edge
// Timer3 Overflow Interrupt: Off
// Input Capture Interrupt: Off
// Compare A Match Interrupt: On
// Compare B Match Interrupt: Off
// Compare C Match Interrupt: Off
TCCR3A=0x00;
TCCR3B=0x08;
TCNT3H=0x00;
TCNT3L=0x00;
ICR3H=0x00;
ICR3L=0x00;
OCR3AH=0xF4;
OCR3AL=0x23;
OCR3BH=0x00;
OCR3BL=0x00;
OCR3CH=0x00;
OCR3CL=0x00;

// Timer/Counter 4 initialization
```

```
// Clock source: System Clock
// Clock value: 7.813 kHz
// Mode: CTC top=OCR4A
// OC4A output: Discon.
// OC4B output: Discon.
// OC4C output: Discon.
// Noise Canceler: Off
// Input Capture on Falling Edge
// Timer4 Overflow Interrupt: Off
// Input Capture Interrupt: Off
// Compare A Match Interrupt: On
// Compare B Match Interrupt: Off
// Compare C Match Interrupt: Off
TCCR4A=0x00;
TCCR4B=0x08;
TCNT4H=0x00;
TCNT4L=0x00;
ICR4H=0x00;
ICR4L=0x00;
OCR4AH=0xC6;
OCR4AL=0x5C;
OCR4BH=0x00;
OCR4BL=0x00;
OCR4CH=0x00;
OCR4CL=0x00;

// Timer/Counter 5 initialization
// Clock source: System Clock
// Clock value: 1000.000 kHz
// Mode: CTC top=OCR5A
// OC5A output: Discon.
// OC5B output: Discon.
// OC5C output: Discon.
// Noise Canceler: Off
// Input Capture on Falling Edge
// Timer5 Overflow Interrupt: Off
// Input Capture Interrupt: Off
// Compare A Match Interrupt: On
// Compare B Match Interrupt: Off
// Compare C Match Interrupt: Off


// External Interrupt(s) initialization
// INT0: Off
// INT1: Off
// INT2: Off
// INT3: Off
// INT4: Off
// INT5: Off
// INT6: Off
// INT7: On
// INT7 Mode: Rising Edge

EICRA=0x00;
EICRB=0xC0;
EIMSK=0x80;
EIFR=0x80;

// PCINT0 interrupt: Off
// PCINT1 interrupt: Off
// PCINT2 interrupt: Off
// PCINT3 interrupt: Off
// PCINT4 interrupt: Off
```

```
// PCINT5 interrupt: Off
// PCINT6 interrupt: Off
// PCINT7 interrupt: On
// PCINT8 interrupt: Off
// PCINT9 interrupt: Off
// PCINT10 interrupt: Off
// PCINT11 interrupt: Off
// PCINT12 interrupt: Off
// PCINT13 interrupt: Off
// PCINT14 interrupt: Off
// PCINT15 interrupt: Off
// PCINT16 interrupt: Off
// PCINT17 interrupt: Off
// PCINT18 interrupt: Off
// PCINT19 interrupt: Off
// PCINT20 interrupt: Off
// PCINT21 interrupt: Off
// PCINT22 interrupt: Off
// PCINT23 interrupt: Off
PCMSK0=0x80;
PCMSK1=0x00;
PCMSK2=0x00;
PCICR=0x01;

// Timer/Counter 0 Interrupt(s) initialization
TIMSK0=0x00;

// Timer/Counter 1 Interrupt(s) initialization
TIMSK1=0x03;

// Timer/Counter 2 Interrupt(s) initialization
TIMSK2=0x00;

// Timer/Counter 3 Interrupt(s) initialization
TIMSK3=0x02;

// Timer/Counter 4 Interrupt(s) initialization
TIMSK4=0x02;

// Timer/Counter 5 Interrupt(s) initialization
TIMSK5=0x02;

// USART0 initialization
// Communication Parameters: 8 Data, 1 Stop, No Parity
// USART0 Receiver: Off
// USART0 Transmitter: On
// USART0 Mode: Asynchronous
// USART0 Baud Rate: 9600
UCSR0A=0x00;
UCSR0B=0x08;
UCSR0C=0x06;
UBRR0H=0x00;
UBRR0L=0x67;
stdout = &mystdout; //Used in defining stream for stdio.h functions

// USART1 initialization
// USART1 disabled
UCSR1B=0x00;

// USART2 initialization
// USART2 disabled
UCSR2B=0x00;
```

```
    // USART3 initialization
    // USART3 disabled
    UCSR3B=0x00;

    // Analog Comparator initialization
    // Analog Comparator: Off
    // Analog Comparator Input Capture by Timer/Counter 1: Off
    ACSR=0x80;
    ADCSRB=0x00;
    DIDR1=0x00;

    // ADC initialization
    // ADC Clock frequency: 1000.000 kHz
    // ADC Voltage Reference: AVCC pin
    // ADC Auto Trigger Source: ADC Stopped
    // Digital input buffers on ADC0: On, ADC1: On, ADC2: On, ADC3: On
    // ADC4: On, ADC5: On, ADC6: On, ADC7: On
    DIDR0=0x00;
    // Digital input buffers on ADC8: On, ADC9: On, ADC10: On, ADC11: On
    // ADC12: On, ADC13: On, ADC14: On, ADC15: On
    DIDR2=0x00;
    ADMUX=0x40;
    ADCSRA=0x87;

    // SPI initialization
    // SPI disabled
    SPCR=0x00;

    // TWI initialization
    // TWI disabled
    TWCR=0x00;

    // Global enable interrupts

    sei();

    TCCR1B |= ENABLE_SAMP1;

    //printf("Board reset\n\r");   //Used in debugging

    while (1)
    {

    }
}

//Optional External Interrupt ISR-May be used for pushbutton
ISR(INT7_vect){
}

// Calibration tasks and sampling
// Timer1 output compare A interrupt service routine
// f = 100Hz
ISR(TIMER1_COMPA_vect){
    //Local Variable Definitions
    volatile static uint8_t localmax=0;//used as bools to detect if a point is local
maximum or minimum
    volatile static uint8_t localmin=0;
    volatile static uint8_t minpos=0; //holds location of largest value in initialMIN
    volatile static uint8_t maxpos=0;//holds location of least value in initialMAX

    static uint16_t minstdsum;//used in calculation of standard deviations
    static uint16_t maxstdsum;//used in calculation of standard deviations
```

```
    static uint16_t maxstd;//store standard deviation of max/min values
    static uint16_t minstd;
    static uint16_t minsum = 0;// will hold sum of 8 values in initialMIN
    static uint16_t maxsum = 0;//same for initialMAX
    static uint16_t bin; //this will be used in the bubble sort of the initial arrays
to save a value to swap
    static uint8_t swap = 1; //this will be used as a bool to determine if bubble sort
has completed it's arrangement
    static uint16_t datagrab[5];//holds current input value
    static uint8_t initializema=1;
    static uint8_t debug = 1;
    static uint8_t detected = 0;

    if(initializeinc<=1500){
        initializeinc++;
        resample++;
        if(resample ==10){
            resample = 0;
            for(int i=19; i>=1; i--){
                BREATHDATA[i]=BREATHDATA[i-1];
            }
            BREATHDATA[0] = BREATHFILTER();
            for(int i=5; i>=1; i--){
                datagrab[i]=datagrab[i-1];
            }
            datagrab[0]=BREATHDATA[0];
        }
    }

    if(initializeinc>1500 && initializeinc<4500){

        initializeinc++;
        if(initializema){
            for(int i=7;i>=0;i--){
                initialMAX[i]=1;
                initialMIN[i]=1022;
            }
                for(int i=7;i>=0;i--){
                    datagrab[i]=500;
                }
            initializema=0;
        }

        resample++;
        for(int i=18;i>=1;i--){
            RAWDATA[i]=RAWDATA[i-1];
        }
        RAWDATA[0]=adc_read(1);

        if(resample==10){
            resample = 0;
            for(int i=5; i>=1;i--){
                datagrab[i]=datagrab[i-1];
            }

            datagrab[0] = BREATHFILTER();

            localmax=1;
            localmin=1;
            for(int i=5; i>=1; i--){
                if(datagrab[i]>datagrab[2]){
                    localmax=0;
                }
```

```
                if(datagrab[i]<datagrab[2]){
                    localmin=0;
                }
            }
            if(localmin){//find largest value stored in initialMIN
                for(int i=0;i<=7;i++){
                    if(initialMIN[i]>initialMIN[minpos]){
                        minpos=i;
                    }
                }
            }

                //compare largest value to the new local minimum

            if(datagrab[2]<initialMIN[minpos]){
                    if(datagrab[2]<=5){

                    }
                initialMIN[minpos]=datagrab[2];
            }


            if(localmax){//behaves the same way as min loops, but for replacing the
smallest max value
                for(int i=0;i<=7;i++){
                    if(initialMAX[i]<initialMAX[maxpos]){
                        maxpos=i;
                    }
                }
                if(datagrab[2]>initialMAX[maxpos]){
                    initialMAX[maxpos]=datagrab[2];
                }
            }
        }
    }

    if(initializeinc == 4500){

        initializeinc++;
        for(int i=0;i<=7;i++){//calculate average values of max and min
            maxsum += initialMAX[i];
            minsum += initialMIN[i];
        }

        maxsum /= 8;
        minsum /= 8;

        for(int i=0; i<=7; i++){
            minstdsum += (initialMIN[i]-minsum)^2;
            maxstdsum += (initialMAX[i]-maxsum)^2;
        }

        maxstd = sqrt(maxstdsum/8);
        minstd = sqrt(minstdsum/8);

        for(int i=7;i>=0;i--){
            if(initialMIN[i]<=(minsum-minstd)){
                initialMIN[i]=1022;//if the value is outside the range of standard
deviation, set it high so it will be ignored when the 5 smallest values are taken
            }
            if(initialMAX[i]>=(maxsum+maxstd)){
                initialMAX[i]=1;//set low so it will be ignored
            }
```

```
    }

//bubble sort
    swap=0;
    while(!swap){
        swap=1;
        for(int i=0;i<=6;i++){
            if(initialMAX[i]<initialMAX[i+1]){
                swap=0;
                bin = initialMAX[i];
                initialMAX[i]=initialMAX[i+1];
                initialMAX[i+1] = bin;
            }
        }
    }
    swap = 0;
    while(!swap){
        swap=1;
        for(int i=0;i<=6;i++){
            if(initialMIN[i]>initialMIN[i+1]){
                swap=0;
                bin = initialMIN[i];
                initialMIN[i]=initialMIN[i+1];
                initialMIN[i+1]=bin;
            }
        }
    }
    /*for(int i=0;i<=7;i++){
        printf("%u\n\r",initialMIN[i]);

    }
    for(int i=0;i<=7;i++){
    printf("%u\n\r",initialMAX[i]);
    }*/
    maxsum=0;
    minsum=0;
    for(int i=0; i<=4; i++){
        maxsum +=initialMAX[i];
        minsum +=initialMIN[i];

    }

    maxsum /= 5;
    minsum /= 5;

    deltaave = maxsum-minsum;
    currentmax = 0;
    currentmin = 1023;
    TCCR4B |= ENABLE_ALM4;

}
if(initializeinc==4501){

    /*static uint16_t drift=0;
    drift++;
    if(drift==750){
        currentmax=BREATHDATA[0];
        currentmin=BREATHDATA[0];
    }*/
    MaxTik++;
    MinTik++;
    if(MaxTik==600){
        currentmax=BREATHDATA[0];
```

```
            MaxTik = 0;
        }
        if(MinTik==600){
            currentmin=BREATHDATA[0];
            MinTik = 0;
        }
        threshcount++;
        if(threshcount == 200){
            threshcount=0;
            breaththresh=0;
        }
        RAWDATA[0] = adc_read(1);

        resample++;

        if(resample==10){
            for(int i=19; i>=1; i--){
                BREATHDATA[i]=BREATHDATA[i-1];
            }
            BREATHDATA[0]=BREATHFILTER();

            if(BREATHDATA[0] > currentmax){
                currentmax = BREATHDATA[0];
            }

            if(BREATHDATA[0]<currentmin){
                currentmin = BREATHDATA[0];
            }

            deltacurrent = currentmax-currentmin;
            printf("%u\r\n",deltacurrent);
            if(deltacurrent >= .65*deltaave){
                printf("refreshed");
                currentmin=BREATHDATA[0];
                currentmax = BREATHDATA[0];
                //drift = 0;
                TCNT4 = 0x0000;//reset if there are no problems detected, will include
ecg check at a later date
                alarmcount=0;
            }


            resample = 0;
        }

        /*for(int i=19; i>=1; i--){
            ECGDATA[i]=ECGDATA[i-1];
        }

        ECGDATA[0]=ECGFILTER();
        //putchar(ECGDATA[0]);

        HBcount++;
        if(HBcount>=500){
            countover5 = 1;
        }
        if(HBcount>=150){
            countover15 = 1; //corresponds to 40bpm
        }
        if(ECGDATA[0]>=90){
            //heart led on
```

```
            TCCR3B |= ENABLE_HL3;//enable one shot timer to generate a turn off of led
in .25 seconds
            if(HBcount<=140){
                countover15 = 0;
            }
            HBcount=0;

        }
        */
        //checkALARM();
    }
}

// Timer3 output compare A interrupt service routine
// f = 4Hz
ISR(TIMER3_COMPA_vect){
PORTB &= 0xF7;//turn off heart LED
TCCR3B &= DISABLE_HL3;//disable timer
}

// Timer4 output compare A interrupt service routine
// f = 133.33mHz
ISR(TIMER4_COMPA_vect){
    //used to track number of times alarm generated, 4 = 15s total

    if(alarmcount ==4){
        while(1){
            PORTB |= 0x10;
        }
    }

    if(alarmcount <4){
        alarmcount++;
    }

}

// Read the AD conversion result
uint16_t BREATHFILTER(){
    uint16_t j;
    for(int i=6; i>=1; i--){
        BREATHFILTERSTORAGE[i]=BREATHFILTERSTORAGE[i-1];//shift data to make room for
incoming value
    }
    BREATHFILTERSTORAGE[0]=RAWDATA[0];

    j= (hanningNumCo_b[0] * BREATHFILTERSTORAGE[0] + hanningNumCo_b[1] *
BREATHFILTERSTORAGE[1] +
    hanningNumCo_b[2] * BREATHFILTERSTORAGE[2] + hanningNumCo_b[3] *
BREATHFILTERSTORAGE[3] +
    hanningNumCo_b[4] * BREATHFILTERSTORAGE[4] + hanningNumCo_b[5] *
BREATHFILTERSTORAGE[5] +
    hanningNumCo_b[6] * BREATHFILTERSTORAGE[6]) / hanningDenCo_b[0];
    return(j);
}

uint16_t ECGFILTER(){
    float j = (IIRfiltNumCo[0]*RAWDATA[0] + IIRfiltNumCo[1]*RAWDATA[6] +
    IIRfiltNumCo[2]*RAWDATA[7]+IIRfiltNumCo[3]*RAWDATA[18])/(IIRfiltDenCo[1]*
    IIROUTPUTSTORAGE[0]+IIRfiltDenCo[2]*IIROUTPUTSTORAGE[1] +IIRfiltDenCo[3]*
    IIROUTPUTSTORAGE[2]+IIRfiltDenCo[4]*IIROUTPUTSTORAGE[3] + IIRfiltDenCo[5]*
    IIROUTPUTSTORAGE[4] +IIRfiltDenCo[6]*IIROUTPUTSTORAGE[5]);
```

```
    for(int i=5; i>=1; i--) { //shift values into new spaces in storage array
    IIROUTPUTSTORAGE[i]=IIROUTPUTSTORAGE[i-1];
}
    IIROUTPUTSTORAGE[0] = j;

for(int i=8; i>=1; i--){
    ECGFILTERSTORAGE[i]=ECGFILTERSTORAGE[i-1];//shift data to make room for
                                                //incoming value
}
ECGFILTERSTORAGE[0]=j;//fill newest spot w/ recent value

j = (hanningNumCo_e[0]*ECGFILTERSTORAGE[0] + hanningNumCo_e[1]*ECGFILTERSTORAGE[1] +
hanningNumCo_e[2]*ECGFILTERSTORAGE[2] + hanningNumCo_e[3]*ECGFILTERSTORAGE[3] +
hanningNumCo_e[4]*ECGFILTERSTORAGE[4] + hanningNumCo_e[5]*ECGFILTERSTORAGE[5] +
hanningNumCo_e[6]*ECGFILTERSTORAGE[6] + hanningNumCo_e[7]*ECGFILTERSTORAGE[7] +
hanningNumCo_e[8]*ECGFILTERSTORAGE[8])/hanningNumCo_e[0]; //hanning filter

return(j);
}


uint16_t adc_read(uint8_t ch)
{
    cli();

    // select the corresponding channel 0~7
    // ANDing with '7' will always keep the value
    // of 'ch' between 0 and 7
    ch &= 0x07;  // AND operation with 7 clears superfluous bits
    ADMUX = (ADMUX & 0xF8)|ch;//sets channel
    ADMUX |=(1<<REFS0);
    ADCSRB &=0x00;


    // start single conversion
    // write '1' to ADSC
    ADCSRA |= (1<<ADSC);

    // wait for conversion to complete
    // ADSC becomes '0' again
    // till then, run loop continuously
    while(ADCSRA & (1<<ADSC)){};

    sei();
    return (ADC);
}

//This function is used to build all stdio.h functions
static int uart_putchar(char c, FILE  *stream)
{
    while ( !( UCSR0A & (1<<UDRE0)) ){
    }
    UDR0 = c;
    return 0;
}

void checkALARM(){
    countover15 = 0;
    if(!countover15 && breaththresh){

        TCNT4 = 0x0000;//reset if there are no problems detected
        alarmcount=0;
    }
```

```
    if(countover5){
        alarmcount=1;
        TCNT4 = 0xC65B;//sets timer one tick before compare match, generating an
overflow functionally immediately
    }

    return;
}
```